

# Predefined Time Prescribed Performance Backstepping Control for Robotic Manipulators with Input Saturation

Shuli Liu<sup>1,2</sup>, Yi Liu<sup>3\*</sup>, Jingang Liu<sup>3\*</sup>, Yin Yang<sup>1,2\*</sup>

<sup>1</sup>School of Mathematics and Computational Science, Xiangtan University, Street, City, 411105, China.

<sup>2</sup>National Center for Applied Mathematics in Hunan, Street, City, 411105, China.

<sup>3</sup>School of Mechanical Engineering and Mechanics, Xiangtan University, Street, City, 411105, China.

\*Corresponding author(s). E-mail(s): [liuyi\\_hust@163.com](mailto:liuyi_hust@163.com); [wellbuild@126.com](mailto:wellbuild@126.com); [yangyinxtu@xtu.edu.cn](mailto:yangyinxtu@xtu.edu.cn);  
Contributing authors: [shunnee@163.com](mailto:shunnee@163.com);

## 摘要

For robotic manipulators trajectory tracking with unknown dynamics, bounded disturbances, and input saturation, this work proposes an adaptive backstepping control method that combines predefined time convergence with global predefined performance constraints. A channel-wise predefined-time error transformation merges a polynomial performance function with error scaling. It removes initial-state singularities and nonsmooth mappings in conventional PPC and enforces strict, smooth, global bounds within a user-set time, even from unknown initial states. We also design a unified saturation compensator that cancels residuals from command filtering and actuator saturation, curbs the backstepping complexity explosion, and reduces online computation. A first-order sliding-mode disturbance observer and an RBFNN estimator run online to handle bounded disturbances and unmodeled dynamics. With predefined-time stability theory and an adaptive dynamic barrier Lyapunov function, we prove closed-loop boundedness and on-time convergence. Simulations and experiments show faster response, better steady-state accuracy, and stronger robustness than existing methods.

**Keywords:** Prescribed performance control, predefined-time stability, adaptive dynamic barrier Lyapunov function, backstepping control, input saturation, robotic manipulators' trajectory tracking.

## 1 Introduction

机器人机械臂凭借其高精度和柔性特性，广泛应用于工业装配、航天探测、医疗手术等高要求场景 [1, 2]。机械臂通常需要在有限时间内完成高精度轨迹跟踪，其动力学系统常伴随强非线性、多输入多输出耦合及显著不确定性，且常伴随有界扰动与执行器饱和 [1, 3]。若控制不当，极易导致误差放大、响应迟缓，甚至系统失稳。在不确定条件下实现整个轨迹跟踪过程中误差的有效约束，并使其在严格规定的时间内收敛，是当前控制研究的重要问题。围绕上述目标，研究者们已提出诸多控制策略，包括PID反馈控制 [2, 4]、自适应控制 [5–7]、滑模控制 [8–10]、模型预测控制 [11]、强化学习控制 [12, 13] 等。然而，传统渐近型方法难以保证收敛时限，且对误差边界与饱和的显式约束不足。

为缓解上述不足，利用神经网络（NN）[14]、模糊逻辑系统（FLS）[15]和自适应法则[16]对未知非线性进行实时逼近。基于扰动观测器的补偿控制、高阶滑模控制以及边界层等技术被广泛引入。众所周知，传统渐近稳定控制方法在理论上的收敛时间可能无限长，难以满足实际应用对快速动态响应的严格需求 [17]。因此，有限时间控制(Finite-Time Control, FTC)理论逐渐引入，实现非线性系统的快速稳定控制 [18–20]。然而，这类控制方案的收敛特性依赖初始条件，初始误差较大时收敛时间显著延长，难以满足严格的时域控制要求。针对收敛时间不可预测的问题，学者们提出了固定时间控制(FxTC)确保系统收敛时间的上界独立于初始状态，解决初始条件带来的收敛时间不确定性问题 [21]。但其收敛时间上界完全由控制参数决定，无法由用户直接指定特定的收敛时

刻 [9, 22]。为克服这一局限, related work 提出了预定义时间稳定性理论, 在控制器中显式引入收敛时间参数, 使得收敛时间上界能够由用户任意设定, 且与初始条件无关 [23–25]。PTC在对时域性能要求严格的电力系统与机器人控制等领域中迅速获得广泛关注 [25–28]。

另一方面, 为严格限定轨迹跟踪过程中的瞬态性能与稳态精度, 预设性能控制 (PPC) 通过误差映射确保误差始终处于设计包络内, 可显著抑制超调并提升收敛质量 [29, 30]。实质上, PPC提供了一种系统化的预规划机制, 确保运行过程中跟踪误差被严格约束在设计指标范围内 [31–33]。与势垒李雅普诺夫函数 (BLFs) 结合可进一步提升安全性与鲁棒性 [34, 35]。该方法及其变种已被成功应用于机器人及其他非线性系统[36, 36–38]。然而, 误差变换在边界附近可能奇异或非光滑, 且常隐含要求初始误差位于包络内, 难以处理高速冲击的工程问题。且传统PPC与BLF方法往往仅保证误差渐近收敛, 缺乏时间收敛控制能力。近期研究开始探索将预设性能与有限时间控制相结合, 以兼顾收敛质量与时间指标 [14, 39–42]。例如, Liu 等提出了基于PPC的自适应神经网络有限时间控制方案 [14]; Zhang 等设计了具有全局有限时间稳定性的自适应PPC策略, 应用于机械臂跟踪控制 [8]。与此同时, 有相关工作将固定时间控制与预设性能约束结合 [22, 43–46]。例如, Zhou 等提出了一种用于参数时变非线性系统的固定时间PPC控制方案 [45], Yang 等设计了具备PPC功能的近似固定时间容错跟踪控制策略 [9, 46], Zhang 等开发了适用于机器人系统的全局复合学习固定时间控制框架, 并引入非对称误差约束 [22]。然而, 这些方法对初始条件仍敏感, 难以确保在大初值误差条件下快速满足预期性能, 且无法显式设置收敛时限。

尽管已有少量work开始探索PTC与PPC相结合, 但整体上仍缺乏统一完备的理论框架。例如, Wang 等围绕非合作航天器接管任务给出了非奇异预定义时间终端滑模与新型性能函数, 实现姿态误差的定量约束 [47]; Yao 等针对带输入时延的随机非线性系统提出了基于PTC与性能函数的切换误差变换, 突破了传统 PPC 需将初值置于包络内的限制 [48]; Liu 等将模糊自适应与预定义时间性能函数结合, 获得在不确定扰动下的全局 PPC 控制 [15]。但这些研究普遍未系统纳入执行器饱和与关节速度显式约束。实际中, 若饱和非线性处理不当, 轻则性能显著劣化, 重则诱发超调甚至失稳。更关键的是, 性能约束与状态/输入饱和能力约束相互耦合, 收紧边界会推高控制需求并触发饱和, 而饱和又可能逼迫误差逼近或跨越边界。近年来有相关工作提出柔性PPC, 在接近饱和时临时放宽边界、脱离后再收紧, 以在线权衡可实现性与性能 [49, 50]。另一方面, 安全动态包络增强的 PPC 通过饱和检测与安全域调度抑制边界与饱和的相互激化 [51]。也有相关工作提出基于性能函数再调整与抗饱和补偿的等效处理, 将饱和等价为可管控输入并保持 PPC 的约束优势 [52, 53]。尽管如此, 现有方法仍少有在同一框架内同时实现用户可设的预定义时间收敛与全过程性能约束, 并以显式且低复杂度的方式处理饱和问题。

基于上述挑战, 本文提出一种融合预定义时间稳定性与预设性能约束的自适应反步控制方法.主要贡献如下: (i) 按通道独立的预定义时间误差变换, 将多项式性能函数与误差缩放耦合, 系统性消除 PPC 中的初值奇异与非光滑问题, 实现对未知初态的平滑合法化与严格控时的全过程约束; (ii) 设计统一的预定义时间饱和补偿器, 同时抵消命令滤波与执行器饱和残差, 抑制反步结构复杂性爆炸, 降低在线计算与增益需求; (iii) 采用一阶滑模扰动观测器补偿有界扰动与 RBFNN 在线辨识补偿未建模动态; (iv) 基于预定义时间稳定性与自适应动态障碍 Lyapunov 工具, 严格证明闭环系统在预设时间内的全局稳定与误差收敛。多自由度机械臂平台的仿真与实验验证显示, 所提方法在大初始偏差在预定义时间内达成性能约束以及扭矩需求与抖振抑制方面, 均优于对比控制策略, 体现良好的理论可推广性与工程可实施性。

## 2 Problem and preliminary

### 2.1 System description

This work considers an uncertain nonlinear n-DOF robot manipulators system. Its dynamics are described as [1, 2]:

$$M(q)\ddot{q} + C(q, \dot{q})\dot{q} + G(q) + \Delta(q, \dot{q}, t) = \tau + d(t), \quad (1)$$

where  $q, \dot{q}, \ddot{q} \in \mathbb{R}^n$  are the joint state vectors,  $M(q) \in \mathbb{R}^{n \times n}$  is the inertia matrix,  $C(q, \dot{q}) \in \mathbb{R}^{n \times n}$  represents the centrifugal effects,  $G(q) \in \mathbb{R}^n$  represents the gravitational force,  $\tau \in \mathbb{R}^n$  is the control joint input,  $\Delta(q, \dot{q}, t) \in \mathbb{R}^n$  is the uncertainty and unmodeled dynamics,  $d(t) \in \mathbb{R}^n$  is an external disturbance,  $n$  is the number of DOF of the manipulators system.

For controller design, define the state  $x = [x_1^\top, x_2^\top]^\top = [q^\top, \dot{q}^\top]^\top \in \mathbb{R}^{2n}$ . The system eq. (1) can be written in the standard state space form:

$$\begin{cases} \dot{x}_1 = x_2, \\ \dot{x}_2 = f + g\bar{u} + h, \end{cases} \quad (2)$$

where  $f = -M^{-1}(q)(C(q, \dot{q})x_2 + G(q))$ ,  $g = M^{-1}(q)$ ,  $h = -M^{-1}(q)(\Delta(q, \dot{q}, t) - d(t))$ , and  $x_1 = [x_{1,1}, x_{2,1}, \dots, x_{n,1}]^\top$ ,  $x_2 = [x_{1,2}, x_{2,2}, \dots, x_{n,2}]^\top$ ,  $\bar{u}$  denotes control input saturation. Define the saturation error as

$$\Delta u_i = u_i - \bar{u}_i = \begin{cases} u_i - u_{\max}, & u_i \geq u_{\max}, \\ 0, & u_{\min} < u_i < u_{\max}, \\ u_i - u_{\min}, & u_i \leq u_{\min}, \end{cases} \quad i = 1, 2, \dots, n, \quad (3)$$

where  $u_{\max}, u_{\min}$  are the upper and lower saturation bounds of control input, respectively.

The controller design and stability analysis are conducted under the following physically justified assumptions.

**Assumption 1** [3]  $M(q)$  is symmetric positive definite for all  $q$ . There exist constants  $m_1, m_2 > 0$  such that  $m_1 I \leq M(q) \leq m_2 I$ ,  $\forall q \in \mathbb{R}^n$ . Moreover, the standard structural property holds:  $\dot{M}(q) - 2C(q, \dot{q})$  is skew-symmetric.

**Assumption 2** The unmodeled dynamics are bounded: there exists  $\bar{\Delta} > 0$  such that  $\|\Delta(q, \dot{q}, t)\| \leq \bar{\Delta}$ ,  $\forall t \geq 0$ . The disturbance and its derivative are bounded: there exist  $\bar{d}, \bar{\dot{d}} > 0$  such that  $\|d(t)\| \leq \bar{d}$  and  $\|\dot{d}(t)\| \leq \bar{\dot{d}}$ ,  $\forall t \geq 0$ . The desired trajectory  $q_d(t)$  is twice continuously differentiable, and there exist  $\bar{q}_d, \bar{\dot{q}}_d, \bar{\ddot{q}}_d > 0$  such that  $\|q_d(t)\| \leq \bar{q}_d$ ,  $\|\dot{q}_d(t)\| \leq \bar{\dot{q}}_d$ ,  $\|\ddot{q}_d(t)\| \leq \bar{\ddot{q}}_d$ ,  $\forall t \geq 0$ .

## 2.2 Preliminary

RBFNN is a universal approximator on compact sets and is widely employed to estimate unknown nonlinear functions [26, 41]. The input to the RBFNN is defined as  $\chi$ , the output of the network denoted as  $h_i$ , is expressed as

$$h_i = w_i^{*T} Q_i(\chi) + \varepsilon_i, \quad (4)$$

where  $w_i^* \in \mathbb{R}^N$ ,  $w_i^* = [w_{i,1}, w_{i,2}, \dots, w_{i,N}]^T$  is the idea weight vector,  $Q_i(\chi) \in \mathbb{R}^N$  is the vector of basis functions, and  $\varepsilon_i$  is the approximation error satisfying  $|\varepsilon_i| \leq \bar{\varepsilon}$  for all  $\chi$  in a compact set  $\Omega_\chi \subset \mathbb{R}^m$ , with a known constant  $\bar{\varepsilon} > 0$ .  $Q_i(\chi) = [Q_{i,1}(\chi), Q_{i,2}(\chi), \dots, Q_{i,N}(\chi)]^T$  is the activation function of the hidden layer neurons. The base function  $Q_{i,\ell}(\chi)$  is

$$Q_{i,\ell}(\chi) = \exp\left(-\frac{\|\chi - o_\ell\|^2}{D_\ell^2}\right), \quad \ell = 1, 2, \dots, N, \quad (5)$$

where  $o_\ell \in \mathbb{R}^m$  and  $D_\ell > 0$  denote the center and width of the Gaussian basis, respectively;  $N$  is the number of neurons.

Let  $\hat{w}_i$  be the adaptive estimate of  $w_i^*$  and define the weight estimation error  $\tilde{w}_i = w_i^* - \hat{w}_i$ . The ideal weight  $w_i^*$  is understood as the best fixed parameter within the chosen basis that minimizes the worst-case approximation error over  $\Omega_\chi$ :

$$w_i^* = \arg \min_{w_i \in \mathbb{R}^N} \left\{ \sup_{\chi \in \Omega_\chi} |f_i(\chi) - w_i^\top Q_i(\chi)| \right\}. \quad (6)$$

**Assumption 3** The optimal weight vector  $w_i^*$  is bounded, and there exists  $\|w_i^*\| \leq \bar{w}$ ,  $\bar{w} > 0$ .

**Lemma 1** [25] (Predefined time stable theory). Consider the system  $\dot{x}(t) = f(x(t))$ ,  $x(0) = x_0$ , where  $x \in \mathbb{R}^n$  is the system's state, and  $x(0) = x_0$  is the initial state.  $f(\cdot)$  is continuous and satisfies  $f(0) = 0$ . Let  $V : \mathbb{R}^n \rightarrow \mathbb{R}_+$  be continuously differentiable, positive definite, and radially unbounded, with  $V(0) = 0$  and  $V(x) > 0$  for all  $x \neq 0$ . For given design parameters  $0 < \eta < 1$ ,  $T_p > 0$ , and  $0 < \varsigma < \infty$ , suppose the closed-loop system satisfies

$$\dot{V}(x) \leq -\frac{\pi}{\eta T_p} \left( V(x)^{1-\frac{\eta}{2}} + V(x)^{1+\frac{\eta}{2}} \right) + \varsigma, \quad (7)$$

Then the origin is predefined-time stable with convergence time bounded by  $T_p$ . Moreover,

$$\left\{ \lim_{t \rightarrow T_p^-} x | V \leq \min \left\{ \left( \frac{2\eta T_p \varsigma}{\pi} \right)^{\frac{1}{1-\frac{\eta}{2}}}, \left( \frac{2\eta T_p \varsigma}{\pi} \right)^{\frac{1}{1+\frac{\eta}{2}}} \right\} \right\}, \quad (8)$$

In particular, if  $\varsigma = 0$  then  $V(T_p) = 0$ .

**Lemma 2** [54] For  $\mathcal{X}, \mathcal{Y} \geq 0$ , and  $\mathcal{Z}_1, \mathcal{Z}_2 > 1$  with  $1/\mathcal{Z}_1 + 1/\mathcal{Z}_2 = 1$ , the following inequalities hold:

$$\mathcal{X}\mathcal{Y} \leq \frac{\mathcal{X}^{\mathcal{Z}_1}}{\mathcal{Z}_1} + \frac{\mathcal{Y}^{\mathcal{Z}_2}}{\mathcal{Z}_2}, \quad (9)$$

Moreover, for any  $\mathcal{Z}_1, \mathcal{Z}_2 > 0$  with  $\mathcal{Z}_1 + \mathcal{Z}_2 = 1$  and any  $\mathcal{Z}_3 > 0$  (generalized weighted form),

$$|\mathcal{X}|^{\mathcal{Z}_1} |\mathcal{Y}|^{\mathcal{Z}_2} \leq \mathcal{Z}_1 \mathcal{Z}_3^{-\frac{\mathcal{Z}_2}{\mathcal{Z}_1}} |\mathcal{X}| + \mathcal{Z}_2 \mathcal{Z}_3 |\mathcal{Y}|. \quad (10)$$

**Lemma 3** [55] Let  $\mathcal{X}_i \in \mathbb{R}$  and  $\mathcal{Y} \in \mathbb{R}^+$ . Then

$$\sum_{i=1}^n |\mathcal{X}_i|^\mathcal{Y} \geq \left( \sum_{i=1}^n |\mathcal{X}_i| \right)^\mathcal{Y}, \quad \mathcal{Y} \in (0, 1), \quad (11)$$

$$\sum_{i=1}^n |\mathcal{X}_i|^\mathcal{Y} \geq n^{1-\mathcal{Y}} \left( \sum_{i=1}^n |\mathcal{X}_i| \right)^\mathcal{Y}, \quad \mathcal{Y} \in (1, \infty). \quad (12)$$

**Lemma 4** [56] For  $\mathcal{Y} > 0$ ,  $\mathcal{X} \in \mathbb{R}$  with  $|\mathcal{X}| < \mathcal{Y}$ , there is

$$\log \left( \frac{\mathcal{Y}^2}{\mathcal{Y}^2 - \mathcal{X}^2} \right) \leq \frac{\mathcal{X}^2}{\mathcal{Y}^2 - \mathcal{X}^2}. \quad (13)$$

### 3 Predefined time error transformation function

为同时化解初值越界奇异性、实现全局动态误差约束与轨迹跟踪误差在预设时间内的合法压缩与稳定收敛，本文设计了一个新的误差变换结构。其性能函数定义如下：

$$\rho(t) = a + (\rho_0 - a) \sum_{i=0}^4 \nu_i B_{i,4}(b), \quad \nu_0 = 1 > \nu_1 > \dots > \nu_4 = 0, \quad (14)$$

其中  $b = (t/T_p)^p \in [0, 1]$  为归一化时间,  $T_p > 0$  为预定义收敛时间,  $0 < p < 1$  控制初期压缩速度,  $\rho_0$  和  $a$  分别为初始误差和稳态误差, 四次Bernstein 基函数满足  $\sum_{i=0}^4 B_{i,4}(b) = 1, 0 \leq B_{i,4}(b) \leq 1$ .

From eq. (14),  $\rho(t)$  具有以下数学性质：(i)  $\rho(0) = \rho_0, \rho(T_p^-) = \rho(T_p^+) = a$ . (ii)  $\rho(t)$  严格单调递减,  $\dot{\rho}(t) < 0$ . (iii)  $\rho(t)$  在  $t \in [0, +\infty)$  上均连续可导.  $\rho(t)$  的时间导数如下：

$$\dot{\rho}(t) = -4(\rho_0 - a) \sum_{i=0}^3 (\nu_i - \nu_{i+1}) B_{i,3}(b) \dot{b}, \quad (15)$$

where  $\dot{b} = p/T_p (t/T_p)^{p-1} > 0$ .

为了实现误差动态调制, 设计一种具有形状可调性的新型误差缩放函数, 定义如下:

$$\beta(t) = \begin{cases} \frac{1}{I(v_1, v_2)} \int_0^b u^{v_1-1} (1-u)^{v_2-1} du, & t \in [0, T_p], \\ 1, & t \in [T_p, +\infty), \end{cases} \quad (16)$$

其中,  $v_1 > 1, v_2 > 1$  为形状参数,  $I(v_1, v_2) = \int_0^1 u^{v_1-1} (1-u)^{v_2-1} du$  为归一化因子, 使得  $\beta : [0, T_p] \rightarrow [0, 1]$ . From eq. (16), we get

$$\lim_{t \rightarrow T_p^-} \beta(t) = \lim_{t \rightarrow T_p^+} \beta(t) = 1, \quad (17a)$$

$$\lim_{t \rightarrow T_p^-} \dot{\beta}(t) = \lim_{t \rightarrow T_p^+} \dot{\beta}(t) = 0 \text{fi} \quad (17b)$$

其中  $t \rightarrow T_p^-$  时, 因  $(1-b)^{v_2-1} \rightarrow 0$  ( $v_2 > 1$ ), 导数自然趋零。 $\beta(t)$  的显式导数为:

$$\dot{\beta}(t) = \begin{cases} \frac{1}{I(v_1, v_2)} \dot{b} b^{v_1-1} (1-b)^{v_2-1}, & t \in [0, T_p) \\ 0, & t \in [T_p, +\infty). \end{cases} \quad (18)$$

From eqs. (16) and (17),  $\beta(t)$  具有以下数学性质: (i)  $\beta(0) = 0$ ,  $\beta(T_p) = 1$ ; (ii)  $\dot{\beta}(t) > 0$ ,  $\beta(t)$  严格单增; (iii)  $\beta$  在  $[0, \infty)$  上  $C^1$  (在  $t = T_p$  左右导数一致为 0)。

定义缩放误差为:

$$z(t) = \beta(t) e(t), \quad t \in [0, T_p) \quad (19)$$

其中  $e(t)$  为原始跟踪误差。该构造满足  $z(0) = 0 < \rho_0$ , 即便  $|e(0)| > \rho(0)$  也保证 Lyapunov 初值有限并避免初值奇异性; 受控下的约束被转写为  $|z(t)| < \rho(t)$ ; 当  $t \geq T_p$  时  $\beta(t) = 1$ ,  $\rho(t) = a$ , 约束自然退化为稳态精度界  $|e(t)| < a$ 。  $z(t)$  在控制器设计中作为替代误差输入, 嵌入 Lyapunov 函数与反馈控制律中。

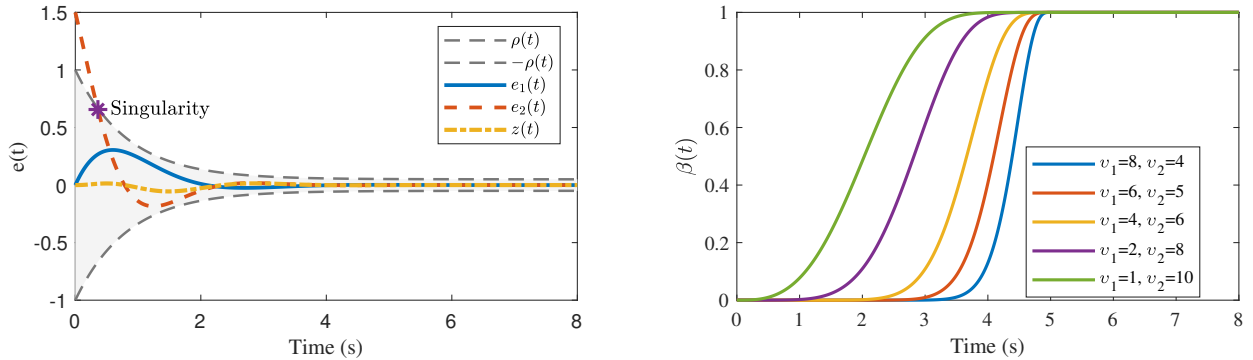


图 1 Error shift transformation and shift function.

*Remark 1* 如 fig. 1 所示: 左图给出了经移位变换后的缩放误差轨迹  $z(t)$  相对于性能包络  $\rho(t)$  的演化。即便存在  $|e(0)| > \rho(0)$  的初值越界, 由于  $\beta(0) = 0$  从而  $z(0) = 0$ , 误差在变量层面被“强制合法化”, 避免了传统 PPC 采用  $z = e/\rho$  时在进入阶段出现的奇异性与可行域切换 (往往需要投影算子或非对称放缩等权宜修补)。右图展示了不同形状参数  $(v_1, v_2)$  下的  $\beta(t)$  曲线族, 体现出“前期更缓/更陡、后期更快/更慢”的可调缩放能力, 可在力矩峰值与稳态精度之间进行显式权衡。综合来看, 本文的误差变换结构的特点在于: (i) 将预定义时间的边界收紧 (Bernstein 加权的  $\rho$ ) 与误差注入路径成形解耦成双调谐器, 实现预定义时间+预设性能的可设计收敛路径; (ii) 通过  $z(0) = 0$  从源头消除初值奇异性与非法区问题, 无需额外重置/投影机制; (iii)  $\dot{\rho}(t), \dot{\beta}(t)$  具备封闭、光滑、可界的解析形式, 便于与饱和补偿、RBFNN 等模块级联并保持 Lyapunov 证明闭合。

## 4 Main results

In a trajectory tracking control system, to guarantee that tracking error meets the prescribed dynamic and steady-state performance requirements, define the tracking error as

$$e_1 = x_1 - q_d - \zeta_1, \quad (20a)$$

$$e_2 = x_2 - \alpha^f - \zeta_2, \quad (20b)$$

where  $\alpha$  is the virtual control,  $\bar{\alpha}$  denotes its elementwise saturation,  $\alpha^f$  is a filtered version of  $\bar{\alpha}$ , and  $\zeta_1, \zeta_2 \in \mathbb{R}^n$  are dynamic anti-saturation compensators of virtual and actual channels, respectively.

## 4.1 饱和补偿器构造

Define the difference between the commanded and saturated signals is the virtual saturation residue  $\Delta\alpha_i$  as follows:

$$\Delta\alpha_i \triangleq \alpha_i - \bar{\alpha}_i = \begin{cases} \alpha_i - \alpha_{\max}, & \alpha_i \geq \alpha_{\max}, \\ 0, & \alpha_{\min} < \alpha_i < \alpha_{\max}, \\ \alpha_i - \alpha_{\min}, & \alpha_i \leq \alpha_{\min}, \end{cases} \quad (21)$$

where  $\alpha_{\max}, \alpha_{\min}$  are the bounds of the virtual input.

To smooth the signal and facilitate the design of the subsequent control law, the filter of the virtual controller  $\alpha^f$  is introduced with the following dynamic equations:

$$\dot{\alpha}^f = -\lambda(\alpha^f - \bar{\alpha}), \quad \alpha^f(0) = \bar{\alpha}(0), \quad (22)$$

where  $\lambda > 1$  is the filtering bandwidth. Define the filtering error

$$\tilde{\alpha} = \bar{\alpha} - \alpha^f, \quad (23)$$

From eqs. (21) and (22), its dynamics satisfy  $\dot{\tilde{\alpha}} = \frac{d}{dt}\dot{\alpha} - \lambda\tilde{\alpha}$ .

Since  $\alpha_i$  and  $u_i$  may exceed their limits when the initial error is large, two dynamic compensators  $\zeta_{i,1}, \zeta_{i,2}$  are introduced to pump out the saturation residue within a designer-given time  $T_\zeta < T_p$ ,  $T_\zeta = cT_p$  ( $0 < c < 1$ ),  $T_\zeta$  is the time required for saturation compensation. The dynamic equations for  $\zeta_{i,1}, \zeta_{i,2}$  are designed as follows:

$$\dot{\zeta}_{i,1} = \delta_{i,1} - \mu_1\zeta_{i,1} + \alpha^f - \alpha_i + \zeta_{i,2}, \quad (24a)$$

$$\dot{\zeta}_{i,2} = \delta_{i,2} - \mu_2\zeta_{i,2} - g_i\Delta u_i \quad (24b)$$

where  $\delta_{i,j} = -\pi/(2\gamma T_\zeta)(|\zeta_{i,j}|^{1-\gamma} + |\zeta_{i,j}|^{1+\gamma})$ , ( $j = 1, 2$ ),  $0 < \gamma < 1$ ,  $\mu_1 > 0$ ,  $\mu_2 > 0$ , and  $\zeta_{i,1}(0) = 0$ ,  $\zeta_{i,2}(0) = 0$ . The power-type damping  $\delta_{i,j}$  guarantees predefined-time decay of  $\zeta_{i,j}$  by  $T_\zeta$ , ensuring that saturation residues are fully removed before the main BLF stage tightens to  $T_p$ .

*Remark 2* 传统饱和补偿多采用线性泄放 (如  $-\lambda\zeta + \Delta$ ), 只能指数收敛, 无法对饱和残差清除时间给出硬时限; 本文在 backstepping-BLF 框架中引入双通道、预定义时间的饱和补偿器  $\zeta_1, \zeta_2$ : (i) 通过  $\delta_{i,j}$  的幂律项为饱和残差提供可设计的清除时限  $T_\zeta = cT_p$ , 从而在 Lyapunov 证明中先验地摘除饱和影响; (ii) 在虚拟与实际两级分别补偿  $\Delta\alpha, \Delta u$ , 解耦滤波滞后、输入饱和与主误差通道, 避免传统  $z = e/\rho$  或对数/有理型 BLF 的初值奇异与导数复杂问题.

## 4.2 Controller design

In the first step, a BLF is used as an energy function for the error dynamics. We choose:

$$V_1 = \frac{1}{2\omega_1} \sum_{i=1}^n \ln \frac{\rho_{i,1}^2}{\rho_{i,1}^2 - z_{i,1}^2}. \quad (25)$$

where  $\omega_j > 0$  is an adaptive gain. Its adaptation law is

$$\dot{\omega}_j = \begin{cases} -\vartheta V_j, & \omega_{\min} < \omega_j < \omega_{\max}, \\ \max(0, -\vartheta V_j), & \omega_j = \omega_{\min}, \\ \min(0, -\vartheta V_j), & \omega_j = \omega_{\max}, \end{cases} \quad (26)$$

with  $\vartheta > 0$ ,  $0 < \omega_{\min} \leq \omega_j \leq \omega_{\max}$ .

*Remark 3* 由自适应律eq. (26)可知,  $\omega_j$  始终受投影算子约束而保持正数有界, 且单调非增。在大误差阶段加重屏障惩罚、误差减小时自动降权, 比固定权重 BLF 更执行器友好, 并便于与预定义时间项配平。

The time derivation of  $V_1$  yields

$$\dot{V}_1 = -\frac{\dot{\omega}_1}{2\omega_1^2} \sum_{i=1}^n \ln \frac{\rho_{i,1}^2}{\rho_{i,1}^2 - z_{i,1}^2} + \frac{1}{\omega_1} \sum_{i=1}^n \left[ \frac{z_{i,1}\dot{z}_{i,1}}{\rho_{i,1}^2 - z_{i,1}^2} - \frac{\dot{\rho}_{i,1}}{\rho_{i,1}} \frac{z_{i,1}^2}{\rho_{i,1}^2 - z_{i,1}^2} \right]. \quad (27)$$

According to eqs. (19) and (20), one has

$$\dot{z}_{i,1} = \dot{\beta}e_{i,1} + \beta\dot{e}_{i,1} = \dot{\beta}e_{i,1} + \beta(e_{i,2} - \dot{q}_{i,d} + \alpha_i - \delta_{i,1} + \mu_1\zeta_{i,1}), \quad (28)$$

Substituting eq. (28) into eq. (27), and letting  $\Gamma_{i,1} = z_{i,1}/(\rho_{i,1}^2 - z_{i,1}^2)$ , we have

$$\begin{aligned} \dot{V}_1 &= -\frac{\dot{\omega}_1}{2\omega_1^2} \sum_{i=1}^n \ln \frac{\rho_{i,1}^2}{\rho_{i,1}^2 - z_{i,1}^2} + \frac{1}{\omega_1} \sum_{i=1}^n \left[ \frac{z_{i,1}(\dot{\beta}e_{i,1} + \beta\dot{e}_{i,1})}{\rho_{i,1}^2 - z_{i,1}^2} - \frac{\dot{\rho}_{i,1}}{\rho_{i,1}} \frac{z_{i,1}^2}{\rho_{i,1}^2 - z_{i,1}^2} \right] \\ &= -\frac{\dot{\omega}_1}{2\omega_1^2} \sum_{i=1}^n \frac{z_{i,1}^2}{\rho_{i,1}^2 - z_{i,1}^2} + \frac{\Gamma_{i,1}}{\omega_1} \sum_{i=1}^n \left[ \dot{\beta}e_{i,1} + \beta \left( e_{i,2} - \dot{q}_{i,d} + \alpha_i - \delta_{i,1} + \mu_1\zeta_{i,1} - \frac{\dot{\rho}_{i,1}}{\rho_{i,1}} e_{i,1} \right) \right], \end{aligned} \quad (29)$$

To suppress the system error and achieve performance convergence, the virtual control law  $\alpha_i$  is designed as

$$\alpha_i = \dot{q}_{i,d} - e_{i,2} + \delta_{i,1} - \mu_1\zeta_{i,1} + e_{i,1} \left( \frac{\dot{\omega}_1}{2\omega_1} - \frac{\iota_1\dot{\beta}^2 e_{i,1}^2}{\rho_{i,1}^2 - z_{i,1}^2} + \frac{\dot{\rho}_{i,1}}{\rho_{i,1}} - k_{i,1} - \omega_1\Psi_{i,1} \right) - \hat{d}_{i,1} \quad (30)$$

where,  $k_1 = \text{diag}(k_{1,1}, k_{2,1}, \dots, k_{n,1})$ ,  $k_{i,1} > 0$ ,  $\iota_2$ ,  $\Psi_{i,1} = \pi/(2\eta T_p)[1 + (nz_{i,1}\Gamma_{i,1}/2)^{\eta/2}]$  is a regulation term associated with a predefined-time and performance function to achieve convergence regulation of the error.  $\hat{d}_{i,1}$  is a disturbance estimate. Introduce the composite error and the first-order sliding disturbance observer:

$$s_{i,1} = e_{i,2} + v_{i,1}e_{i,1}, \quad v_{i,1} > 0, \quad (31)$$

$$\dot{\hat{d}}_{i,1} = -\bar{h}_{i,1} \text{sgn}(s_{i,1}) - \varpi_{i,1}\hat{d}_{i,1} + \bar{h}_{i,1}\frac{\Gamma_{i,1}}{\omega_1}, \quad (32)$$

where  $\bar{h}_{i,1} > \bar{d}$ ,  $\varpi_{i,1} > \bar{h}_{i,1} + 1$ , and  $\tilde{d}_{i,1} = d_{i,1} - \hat{d}_{i,1}$ .

Since eq. (26),  $\dot{\omega}_j \leq 0$ , one has  $-\dot{\omega}_j/(2\omega_j^2) \geq 0$ . Let  $\iota_j > 0$  Using lemma 4 and Young's inequality gives

$$-\frac{\dot{\omega}_j}{2\omega_j^2} \sum_{i=1}^n \ln \frac{\rho_{i,j}^2}{\rho_{i,j}^2 - z_{i,j}^2} \leq -\frac{\dot{\omega}_j}{2\omega_j^2} \sum_{i=1}^n \frac{z_{i,j}^2}{\rho_{i,j}^2 - z_{i,j}^2}, \quad (33)$$

$$\sum_{i=1}^n \frac{\dot{\beta}e_{i,j}z_{i,j}}{\rho_{i,j}^2 - z_{i,j}^2} \leq \sum_{i=1}^n \frac{\iota_j\dot{\beta}^2 e_{i,j}^2 z_{i,j}^2}{(\rho_{i,j}^2 - z_{i,j}^2)^2} + \frac{n}{4\iota_j}. \quad (34)$$

Furthermore, substituting eqs. (30), (33) and (34) into eq. (29), we obtain

$$\dot{V}_1 \leq -\sum_{i=1}^n \Gamma_{i,1}z_{i,1}\Psi_{i,1} - \frac{1}{\omega_1} \sum_{i=1}^n \left( \frac{k_{i,1}z_{i,1}^2}{\rho_{i,1}^2 - z_{i,1}^2} - \frac{z_{i,1}\hat{d}_{i,1}}{\rho_{i,1}^2 - z_{i,1}^2} \right) + \frac{n}{4\omega_1\iota_1}. \quad (35)$$

The second level BLF candidates are chosen as

$$V_2 = V_1 + \frac{1}{2\omega_2} \sum_{i=1}^n \ln \frac{\rho_{i,2}^2}{\rho_{i,2}^2 - z_{i,2}^2}, \quad (36)$$

The time derivation of  $V_2$  yields

$$\dot{V}_2 = \dot{V}_1 - \frac{\dot{\omega}_2}{2\omega_2^2} \sum_{i=1}^n \ln \left( \frac{\rho_{i,2}^2}{\rho_{i,2}^2 - z_{i,2}^2} \right) + \frac{1}{\omega_2} \sum_{i=1}^n \left[ \frac{z_{i,2}\dot{z}_{i,2}}{\rho_{i,2}^2 - z_{i,2}^2} - \frac{\dot{\rho}_{i,2}}{\rho_{i,2}} \frac{z_{i,2}^2}{\rho_{i,2}^2 - z_{i,2}^2} \right]. \quad (37)$$

From eqs. (2), (19) and (20), one has

$$\dot{z}_{i,2} = \dot{\beta}e_{i,2} + \beta\dot{e}_{i,2} = \dot{\beta}e_{i,2} + \beta(f_i + g_i u_i + h_i - \dot{\alpha}_i^f - \delta_{i,2} + \mu_2\zeta_{i,2}). \quad (38)$$

Substituting eq. (38) into eq. (37), and letting  $\Gamma_{i,2} = z_{i,2}/(\rho_{i,2}^2 - z_{i,2}^2)$  gives

$$\dot{V}_2 = \dot{V}_1 + \sum_{i=1}^n \frac{\beta}{\omega_2} \Gamma_{i,2} \left[ f_i + g_i u_i + h_i - \dot{\alpha}_i^f - \delta_{i,2} + \mu_2 \zeta_{i,2} + e_{i,2} \left( \frac{\iota_2 \dot{\beta}^2 e_{i,2}^2}{\rho_{i,1}^2 - z_{i,2}^2} - \frac{\dot{\omega}_2}{2\omega_2} - \frac{\dot{\rho}_{i,2}}{\rho_{i,2}} \right) \right] + \frac{n}{4\omega_2 \iota_2}, \quad (39)$$

Further, to enforce performance and cancel unknown terms we design the main control law as

$$u_i = g_i^{-1} \left[ -f_i - \hat{h}_i + \dot{\alpha}_i^f + \delta_{i,2} - \mu_2 \zeta_{i,2} + e_{i,2} \left( -\frac{\iota_2 \dot{\beta}^2 e_{i,2}^2}{\rho_{i,1}^2 - z_{i,2}^2} + \frac{\dot{\omega}_2}{2\omega_2} + \frac{\dot{\rho}_{i,2}}{\rho_{i,2}} - k_{i,2} - \omega_2 \Psi_{i,2} \right) - \hat{d}_{i,2} \right], \quad (40)$$

where  $k_2 = \text{diag}(k_{1,2}, k_{2,2}, \dots, k_{n,2})$ ,  $k_{i,2} > 0$ ,  $\iota_2$ ,  $\Psi_{i,2} = \pi/(2\eta T_p)[1 + (nz_{i,2}\Gamma_{i,2}/2)^{\eta/2}]$ .

The unknown dynamics is approximated online by an RBFNN,  $\hat{h}_i = \hat{w}_i^\top Q_i(\chi)$  with input  $\chi = [x_{i,1}, x_{i,2}]^\top$ . The weight adaptation is chosen as

$$\dot{w}_i = \frac{\beta}{\omega_2} \varrho_i Q_i \Gamma_{i,2} - \kappa_i \hat{w}_i, \quad (41)$$

with learning rate  $\varrho_i > 0$  and leakage  $\kappa_i > 0$ .

For disturbance rejection, define the composite sliding signal  $s_{i,2} = e_{i,2} + v_{i,2}e_{i,1}$  ( $v_{i,2} > 0$ ) and employ

$$\dot{\tilde{d}}_{i,2} = -\bar{h}_{i,2} \text{sgn}(s_{i,2}) - \varpi_{i,2} \hat{d}_{i,2} + \bar{h}_{i,2} \frac{\Gamma_{i,2}}{\omega_1}, \quad (42)$$

where  $\bar{h}_{i,2} > \bar{d}$ ,  $\varpi_{i,2} > \bar{h}_{i,2} + 1$ , and  $\tilde{d}_{i,2} = d_{i,2} - \hat{d}_{i,2}$ .

From eqs. (33) to (35), and substituting the control law eq. (40) into eq. (39), we get

$$\begin{aligned} \dot{V}_2 = & - \sum_{i=1}^n \Gamma_{i,1} z_{i,1} \Psi_{i,1} - \frac{1}{\omega_1} \sum_{i=1}^n \frac{k_{i,1} z_{i,1}^2}{\rho_{i,1}^2 - z_{i,1}^2} - \frac{1}{\omega_1} \sum_{i=1}^n \frac{z_{i,1} \hat{d}_{i,1}}{\rho_{i,1}^2 - z_{i,1}^2} \\ & - \sum_{i=1}^n \Gamma_{i,2} z_{i,2} \Psi_{i,2} - \frac{1}{\omega_2} \sum_{i=1}^n \frac{k_{2,i} z_{i,2}^2}{\rho_{2i}^2 - e_{i,2}^2} + \frac{\beta}{\omega_2} \sum_{i=1}^n \Gamma_{i,2} (h_i - \hat{h}_i) \\ & - \frac{1}{\omega_2} \sum_{i=1}^n \frac{z_{i,2} \hat{d}_{i,2}}{\rho_{i,2}^2 - z_{i,2}^2} + \frac{n}{4\omega_1 \iota_1} + \frac{n}{4\omega_2 \iota_2}. \end{aligned} \quad (43)$$

## 5 Stability analysis

We analyze the stability of the closed-loop system under the proposed controller. A composite Lyapunov function eq. (44) is constructed by combining the BLF-based error energy, the RBFNN weight estimation error  $\tilde{w}_i$ , the virtual-control filtering error  $\tilde{\alpha}$ , and the disturbance-estimation errors  $\tilde{d}_{i,1}, \tilde{d}_{i,2}$ . The composite function is able to analyze the trajectory error dynamics, adaptive weight convergence and the preservation of performance constraints in a unified manner. Sufficient conditions for the global stability of the system and for all signals to be bounded are given by the derivation of its time derivative inequality. Ultimately, we show that in any initial state, the system trajectory will converge within a tight set at a set predefined-time  $T_p$ , thus achieving global predefined-time stability.

**Theorem 1** Under Assumptions 1 to 3 and the controller in eqs. (30) and (40) with observers eqs. (32) and (42) and weight update eq. (41), and under certain parameter conditions. At this point, for any initial condition, the closed-loop system is predefined-time stable. The scaled errors  $z_{i,1}(t), z_{i,2}(t)$  enter a compact set no later than  $T_p$ , hence  $|e_i(t)| < \rho_i(t)$  for all  $t$ , and  $e_i(t)$  converges to a prescribed small neighborhood of the origin.

证明 The composite Lyapunov function is constructed as follows

$$V = V_2 + \sum_{i=1}^n \frac{1}{2\varrho_i} \tilde{w}_i^\top \tilde{w}_i + \sum_{i=1}^n \frac{1}{2} \tilde{\alpha}^2 + \sum_{i=1}^n \left( \frac{1}{2\bar{h}_{i,1}} \tilde{d}_{i,1}^2 + \frac{1}{2\bar{h}_{i,2}} \tilde{d}_{i,2}^2 \right). \quad (44)$$

The time derivative of eq. (44) is given by

$$\begin{aligned}\dot{V} = & -\sum_{i=1}^n \Gamma_{i,1} z_{i,1} \Psi_{i,1} - \frac{1}{\omega_1} \sum_{i=1}^n \frac{k_{i,1} z_{i,1}^2}{\rho_{i,1}^2 - z_{i,1}^2} - \frac{1}{\omega_1} \sum_{i=1}^n \frac{z_{i,1} \hat{d}_{i,1}}{\rho_{i,1}^2 - z_{i,1}^2} \\ & - \sum_{i=1}^n \Gamma_{i,2} z_{i,2} \Psi_{i,2} - \frac{1}{\omega_2} \sum_{i=1}^n \frac{k_{2,i} z_{i,2}^2}{\rho_{i,2}^2 - e_{i,2}^2} - \frac{1}{\omega_2} \sum_{i=1}^n \frac{z_{i,2} \hat{d}_{i,2}}{\rho_{i,2}^2 - z_{i,2}^2} \\ & + \frac{\beta}{\omega_2} \sum_{i=1}^n \Gamma_{i,2} (h_i - \hat{h}_i) + \sum_{i=1}^n \frac{1}{\varrho_i} \tilde{w}_i^\top \dot{\tilde{w}}_i + \sum_{i=1}^n \tilde{\alpha} \dot{\alpha} + \sum_{i=1}^n \left( \frac{1}{\hbar_{i,1}} \tilde{d}_{i,1} \dot{\tilde{d}}_{i,1} + \frac{1}{\hbar_{i,2}} \tilde{d}_{i,2} \dot{\tilde{d}}_{i,2} \right) + \frac{n}{4\omega_1 \iota_1} + \frac{n}{4\omega_2 \iota_2}.\end{aligned}\quad (45)$$

Combined with eqs. (4) and (41), we have  $h_i - \hat{h}_i = w_i^{*\top} Q_i - \hat{w}_i^\top Q_i = \tilde{w}_i^\top Q_i$ ,  $\tilde{w}_i = w_i^* - \hat{w}_i$ ,  $\tilde{w}_i^\top \hat{w}_i = \tilde{w}_i^\top w_i - \|\tilde{w}_i\|^2 \leq \bar{w}_i \|\tilde{w}_i\| - \|\tilde{w}_i\|^2$ ,  $\dot{\tilde{w}}_i = -\dot{\hat{w}}_i$ , and combined with Young inequalities  $\bar{w}_i \|\tilde{w}_i\| \leq \frac{1}{2} \|\tilde{w}_i\|^2 + \frac{1}{2} \bar{w}_i^2$ , this yields

$$\begin{aligned}& \frac{\beta}{\omega_2} \sum_{i=1}^n \Gamma_{i,2} (h_i - \hat{h}_i) + \sum_{i=1}^n \frac{1}{\varrho_i} \tilde{w}_i^\top \dot{\tilde{w}}_i \\ &= \frac{\beta}{\omega_2} \sum_i \Gamma_{i,2} \tilde{w}_i^\top Q_i - \sum_i \frac{1}{\varrho_i} \tilde{w}_i^\top \left( -\frac{\beta}{\omega_2} \varrho_i \Gamma_{i,2} Q_i + \kappa_i \hat{w}_i \right) = -\sum_{i=1}^n \frac{\kappa_i}{\varrho_i} \tilde{w}_i^\top \hat{w}_i \\ &= \sum_{i=1}^n \frac{\kappa_i}{\varrho_i} w_i \|\tilde{w}_i\| - \sum_{i=1}^n \frac{\kappa_i}{\varrho_i} \|\tilde{w}_i\|^2 \leq -\frac{\kappa_i}{2\varrho_i} \sum_{i=1}^n \|\tilde{w}_i\|^2 + \frac{\kappa_i}{2\varrho_i} \sum_{i=1}^n \bar{w}_i^2,\end{aligned}\quad (46)$$

From eqs. (22) and (23), the time derivative of the filtering error  $\dot{\alpha}$  is given as

$$\sum_{i=1}^n \tilde{\alpha} \dot{\alpha} = \sum_{i=1}^n \tilde{\alpha} \frac{d}{dt} \bar{\alpha} - \lambda \sum_{i=1}^n \tilde{\alpha}^2, \quad (47)$$

根据eqs. (21) and (23),可知  $\frac{d}{dt} \bar{\alpha}$  为分段连续函数，在整个定义域上仅在两端处存在有限阶不连续点，但整体仍属于 piecewise continuous 函数。虚拟控制律  $\alpha$  是由状态反馈设计得到的连续可导函数，其导数  $\dot{\alpha}$  可由系统状态和参考轨迹导数构成，因此在闭环系统稳定的前提下为有界函数。由此，令  $R_i = \frac{d}{dt} \bar{\alpha}$ ,  $R_i$  是一个有界的连续函数。Then by employing Young's inequality, we obtain:

$$\sum_{i=1}^n \tilde{\alpha} \dot{\alpha} \leq -\frac{\lambda}{2} \sum_{i=1}^n \tilde{\alpha}^2 + \frac{1}{2\lambda} \sum_{i=1}^n R_i^2. \quad (48)$$

In eq. (45), according to lemma 2, and using eqs. (32) and (42),  $\dot{\tilde{d}}_{i,j} = \dot{d}_{i,j} + \hbar_{i,j} \operatorname{sgn}(s_{i,j}) + \varpi_{i,j} \hat{d}_{i,j} - \hbar_{i,j} \Gamma_{i,j} / \omega_j$ . With  $\|\dot{d}_{i,j}\| \leq \bar{d}$  and Young' s inequality, we obtain

$$\frac{1}{\hbar_{i,j}} \tilde{d}_{i,j} \dot{d}_{i,j} \leq \frac{1}{2\hbar_{i,j}} \tilde{d}_{i,j}^2 + \frac{1}{2\hbar_{i,j}} \dot{d}_{i,j}^2, \quad (49a)$$

$$\tilde{d}_{i,j} \operatorname{sgn}(s_{i,j}) \leq \frac{1}{2} \tilde{d}_{i,j}^2 + \frac{1}{2}, \quad (49b)$$

$$\frac{\varpi_{i,j}}{\hbar_{i,j}} \tilde{d}_{i,j} \hat{d}_{i,j} \leq \frac{\varpi_{i,j}}{\hbar_{i,j}} \tilde{d}_{i,j} (d_{i,j} - \tilde{d}_{i,j}) \leq -\frac{\varpi_{i,j}}{2\hbar_{i,j}} \tilde{d}_{i,j}^2 + \frac{\varpi_{i,j}}{2\hbar_{i,j}} \tilde{d}_{i,j}^2, \quad (49c)$$

$$\left| \frac{z_{i,j} d_{i,j}}{\omega_j (\rho_{i,j}^2 - z_{i,j}^2)} \right| \leq \frac{\epsilon_j}{2\omega_j} \frac{z_{i,j}^2}{\rho_{i,j}^2 - z_{i,j}^2} + \frac{1}{2\epsilon_j \omega_j (\rho_{i,j}^2 - z_{i,j}^2)} \tilde{d}_{i,j}^2, \quad (49d)$$

where  $\epsilon_j > 0$  is arbitrary.

Therefore,

$$\begin{aligned}\dot{V}_d = & -\frac{1}{\omega_1} \sum_{i=1}^n \frac{z_{i,1} \hat{d}_{i,1}}{\rho_{i,1}^2 - z_{i,1}^2} - \frac{1}{\omega_2} \sum_{i=1}^n \frac{z_{i,2} \hat{d}_{i,2}}{\rho_{i,2}^2 - z_{i,2}^2} + \sum_{i=1}^n \left( \frac{1}{\hbar_{i,1}} \tilde{d}_{i,1} \dot{\tilde{d}}_{i,1} + \frac{1}{\hbar_{i,2}} \tilde{d}_{i,2} \dot{\tilde{d}}_{i,2} \right) \\ & \leq \left( \frac{1 + \hbar_{i,1} - \varpi_{i,1}}{2\hbar_{i,1}} \right) \tilde{d}_{i,1}^2 + \left( \frac{1 + \hbar_{i,2} - \varpi_{i,2}}{2\hbar_{i,2}} \right) \tilde{d}_{i,2}^2 + \frac{\epsilon_1}{2\omega_1} \frac{z_{i,1}^2}{\rho_{i,1}^2 - z_{i,1}^2} + \frac{\epsilon_2}{2\omega_2} \frac{z_{i,2}^2}{\rho_{i,2}^2 - z_{i,2}^2} + H,\end{aligned}\quad (50)$$

where

$$H = \frac{1}{2\hbar_{i,1}} \tilde{d}_{i,1}^2 + \frac{\varpi_{i,1}}{2\hbar_{i,1}} \tilde{d}_{i,1}^2 + \frac{1}{2\epsilon_1 \omega_1 (\rho_{i,1}^2 - z_{i,1}^2)} \tilde{d}_{i,1}^2 + \frac{1}{2\hbar_{i,2}} \tilde{d}_{i,2}^2 + \frac{\varpi_{i,2}}{2\hbar_{i,2}} \tilde{d}_{i,2}^2 + \frac{1}{2\epsilon_2 \omega_2 (\rho_{i,2}^2 - z_{i,2}^2)} \tilde{d}_{i,2}^2 + 1$$

According to lemma 4, there is

$$\ln \frac{\rho_{i,j}^2}{\rho_{i,j}^2 - z_{i,j}^2} \leq \frac{z_{i,j}^2}{\rho_{i,j}^2 - z_{i,j}^2}. \quad (51)$$

Substituting eqs. (46), (48), (50) and (51) into eq. (45), we get

$$\begin{aligned}\dot{V} &\leq -\frac{1}{\omega_1} \sum_{i=1}^n \frac{k_{i,1} z_{i,1}^2}{\rho_{i,1}^2 - z_{i,1}^2} - \frac{1}{\omega_2} \sum_{i=1}^n \frac{k_{2,i} z_{i,2}^2}{\rho_{2,i}^2 - z_{i,2}^2} - \frac{\kappa_i}{2\varrho_i} \sum_{i=1}^n \|\tilde{w}_i\|^2 - \frac{\lambda}{2} \sum_{i=1}^n \tilde{\alpha}^2 + \left( \frac{1+\hbar_{i,1}-\varpi_{i,1}}{2\hbar_{i,1}} \right) \tilde{d}_{i,1}^2 \\ &+ \left( \frac{1+\hbar_{i,2}-\varpi_{i,2}}{2\hbar_{i,2}} \right) \tilde{d}_{i,2}^2 + \frac{\epsilon_1}{2\omega_1} \frac{z_{i,1}^2}{\rho_{i,1}^2 - z_{i,1}^2} + \frac{\epsilon_2}{2\omega_2} \frac{z_{i,2}^2}{\rho_{i,2}^2 - z_{i,2}^2} + \frac{\kappa_i}{2\varrho_i} \sum_{i=1}^n \bar{w}_i^2 + \frac{1}{2\lambda} \sum_{i=1}^n R_i^2 + \frac{n}{4\omega_1\iota_1} + \frac{n}{4\omega_2\iota_2} + H \\ &\leq \sum_{i=1}^n \left( -\frac{k_{i,1}}{\omega_1} + \frac{\epsilon_1}{2\omega_1} \right) \ln \frac{\rho_{i,1}^2}{\rho_{i,1}^2 - z_{i,1}^2} + \sum_{i=1}^n \left( -\frac{k_{i,2}}{\omega_2} + \frac{\epsilon_2}{2\omega_2} \right) \ln \frac{\rho_{i,2}^2}{\rho_{i,2}^2 - z_{i,2}^2} - \frac{\kappa_i}{2\varrho_i} \sum_{i=1}^n \|\tilde{w}_i\|^2 - \frac{\lambda}{2} \sum_{i=1}^n \tilde{\alpha}^2 \\ &+ \left( \frac{1+\hbar_{i,1}-\varpi_{i,1}}{2\hbar_{i,1}} \right) \tilde{d}_{i,1}^2 + \left( \frac{1+\hbar_{i,2}-\varpi_{i,2}}{2\hbar_{i,2}} \right) \tilde{d}_{i,2}^2 + \frac{\kappa_i}{2\varrho_i} \sum_{i=1}^n \bar{w}_i^2 + \frac{1}{2\lambda} \sum_{i=1}^n R_i^2 + \frac{n}{4\omega_1\iota_1} + \frac{n}{4\omega_2\iota_2} + H.\end{aligned}\quad (52)$$

After organizing eq. (52), the principal negative qualitative and constant bounded terms of Lyapunov's derivative can be obtained, which further leads to

$$\dot{V} \leq -rV + \sigma, \quad (53)$$

with

$$r = \min \left\{ \min_i \left( \frac{2k_{i,1} - \epsilon_1}{\omega_1} \right), \min_i \left( \frac{2k_{i,2} - \epsilon_2}{\omega_2} \right), \min_i (\kappa_i), \lambda, \min_i (\varpi_{i,1} - 1 - \hbar_{i,1}), \min_i (\varpi_{i,2} - 1 - \hbar_{i,2}) \right\} > 0, \quad (54)$$

$$\sigma = \frac{\kappa_i}{2\varrho_i} \sum_{i=1}^n \bar{w}_i^2 + \frac{1}{2\lambda} \sum_{i=1}^n R_i^2 + \frac{n}{4\omega_1\iota_1} + \frac{n}{4\omega_2\iota_2} + H. \quad (55)$$

From the above eqs. (52) to (55), as long as the controller parameters are chosen reasonably,  $V$  is converge exponentially, which implies all signals  $z_{i,1}, z_{i,2}, \tilde{\alpha}, \tilde{w}_i, \tilde{d}_{i,1}, \tilde{d}_{i,2}$  are bounded within the compact set  $\Phi$ . Let

$$\Phi = \left\{ (z_{i,1}, z_{i,2}, \tilde{\alpha}, \tilde{w}_i, \tilde{d}_{i,1}, \tilde{d}_{i,2}) : \| (z, \tilde{\alpha}, \tilde{w}, \tilde{d}) \| \leq \sqrt{\phi} \right\}. \quad (56)$$

According to eqs. (44), (45) and (56), it follows that

$$\begin{aligned}\dot{V} &\leq - \sum_{i=1}^n \Gamma_{i,1} z_{i,1} \left[ \frac{\pi}{\eta T_p} \left( 2^{-1} + n^{\frac{\eta}{2}} 2^{-\frac{\eta}{2}-1} \left( \frac{z_{i,1}^2}{\rho_{i,1}^2 - z_{i,1}^2} \right)^{\frac{\eta}{2}} \right) \right] \\ &- \sum_{i=1}^n \Gamma_{i,2} z_{i,2} \left[ \frac{\pi}{\eta T_p} \left( 2^{-1} + n^{\frac{\eta}{2}} 2^{-\frac{\eta}{2}-1} \left( \frac{z_{i,2}^2}{\rho_{i,2}^2 - z_{i,2}^2} \right)^{\frac{\eta}{2}} \right) \right] \\ &- \frac{\pi}{\eta T_p} \sum_{i=1}^n \left[ \left( \frac{1}{2\varrho_i} \tilde{w}_i^2 \right)^{\frac{\eta}{2}-1} + \left( \frac{1}{2} \tilde{\alpha}^2 \right)^{\frac{\eta}{2}-1} + \left( \frac{1}{2\hbar_{i,1}} \tilde{d}_{i,1}^2 \right)^{\frac{\eta}{2}-1} + \left( \frac{1}{2\hbar_{i,2}} \tilde{d}_{i,2}^2 \right)^{\frac{\eta}{2}-1} \right] \\ &- n^{\frac{\eta}{2}} \frac{\pi}{\eta T_p} \sum_{i=1}^n \left[ \left( \frac{1}{2\varrho_i} \tilde{w}_i^2 \right)^{\frac{\eta}{2}+1} + \left( \frac{1}{2} \tilde{\alpha}^2 \right)^{\frac{\eta}{2}+1} + \left( \frac{1}{2\hbar_{i,1}} \tilde{d}_{i,1}^2 \right)^{\frac{\eta}{2}+1} + \left( \frac{1}{2\hbar_{i,2}} \tilde{d}_{i,2}^2 \right)^{\frac{\eta}{2}+1} \right] \\ &+ \sum_{i=1}^n \frac{2\pi}{\eta T_p} \left[ \left( \frac{\phi}{2} \right)^{1-\frac{\eta}{2}} + n^{\frac{\eta}{2}} \left( \frac{\phi}{2} \right)^{1+\frac{\eta}{2}} \right] + \sigma.\end{aligned}\quad (57)$$

From lemma 2, letting  $\mathcal{X} = 1/2 \sum_{i=1}^n \ln(\rho_j^2 / \rho_j^2 - e_{i,j}^2)$ ,  $\mathcal{Y} = 1$ ,  $\mathcal{Z}_1 = 1 - \eta/2$ ,  $\mathcal{Z}_2 = \eta/2$ ,  $\mathcal{Z}_3 = (\eta/2)^{(n/(2-\eta))}$ , we have

$$\left( \frac{1}{2} \sum_{i=1}^n \ln \frac{\rho_j^2}{\rho_j^2 - e_{i,j}^2} \right)^{1-\frac{\eta}{2}} \leq \frac{1}{2} \sum_{i=1}^n \ln \frac{\rho_j^2}{\rho_j^2 - e_{i,j}^2} + \left( 1 - \frac{\eta}{2} \right) \left( \frac{\eta}{2} \right)^{\frac{\eta}{2-\eta}}. \quad (58)$$

Quoting lemma 3, and combined with eqs. (51) and (58), we get

$$\begin{aligned}\dot{V} &\leq -\frac{\pi}{\eta T_p} \left( \frac{1}{2} \sum_{i=1}^n \ln \frac{\rho_{i,1}^2}{\rho_{i,1}^2 - z_{i,1}^2} + \frac{1}{2} \sum_{i=1}^n \ln \frac{\rho_{2,i}^2}{\rho_{2,i}^2 - z_{i,2}^2} + \sum_{i=1}^n \frac{1}{2\varrho_i} \tilde{w}_i^2 + \sum_{i=1}^n \frac{1}{2} \tilde{\alpha}^2 + \frac{1}{2\hbar_{i,1}} \tilde{d}_{i,1}^2 + \frac{1}{2\hbar_{i,2}} \tilde{d}_{i,2}^2 \right)^{1-\frac{\eta}{2}} \\ &- \frac{\pi}{\eta T_p} \left( \frac{1}{2} \sum_{i=1}^n \ln \frac{\rho_{i,1}^2}{\rho_{i,1}^2 - z_{i,1}^2} + \frac{1}{2} \sum_{i=1}^n \ln \frac{\rho_{2,i}^2}{\rho_{2,i}^2 - z_{i,2}^2} + \sum_{i=1}^n \frac{1}{2\varrho_i} \tilde{w}_i^2 + \sum_{i=1}^n \frac{1}{2} \tilde{\alpha}^2 + \frac{1}{2\hbar_{i,1}} \tilde{d}_{i,1}^2 + \frac{1}{2\hbar_{i,2}} \tilde{d}_{i,2}^2 \right)^{1+\frac{\eta}{2}} \\ &+ \sum_{i=1}^n \frac{2\pi}{\eta T_p} \left[ \left( \frac{\phi}{2} \right)^{1-\frac{\eta}{2}} + n^{\frac{\eta}{2}} \left( \frac{\phi}{2} \right)^{1+\frac{\eta}{2}} \right] + (2-\eta) \left( \frac{\eta}{2} \right)^{\frac{\eta}{2-\eta}} + \sigma \\ &\leq -\frac{\pi}{\eta T_p} \left( V^{1-\frac{\eta}{2}} + V^{1+\frac{\eta}{2}} \right) + \varsigma,\end{aligned}\quad (59)$$

where

$$\varsigma = \sum_{i=1}^n \frac{2\pi}{\eta T_p} \left[ \left( \frac{\phi}{2} \right)^{1-\frac{\eta}{2}} + n^{\frac{\eta}{2}} \left( \frac{\phi}{2} \right)^{1+\frac{\eta}{2}} \right] + (2-\eta) \left( \frac{\eta}{2} \right)^{\frac{\eta}{2-\eta}} + \sigma. \quad (60)$$

In summary, eq. (60) is strictly controlled by the sum of the negative definite term and the bounded term  $\varsigma$ . From lemma 1 then the closed loop system is globally stable at a predefined-time. Remember  $A = [z_1, z_2, \tilde{w}, \tilde{\alpha}, \tilde{d}_1, \tilde{d}_2]^\top \in \mathbb{R}^{6n}$ . And take the Lyapunov function  $V(A) = \|A\|_2^2$ , combined with the previous derivation and eq. (59), it can be seen that, for any initial condition, the closed-loop system globally converges to a compact set  $\Omega$  within a predefined-time  $T_p$ . After that,  $V(A)$  does not increase any further, which ensures that the system remains stable within this set. The  $\Omega$  is as follows

$$\Omega = \left\{ A : \lim_{t \rightarrow T_p} V(A) \leq \min \left\{ \left( \frac{2\eta T_p \varsigma}{\pi} \right)^{\frac{1-\gamma}{2}}, \left( \frac{2\eta T_p \varsigma}{\pi} \right)^{\frac{1+\gamma}{2}} \right\} \right\}. \quad (61)$$

The stability proof is completed.  $\square$

**Theorem 2** Under appropriate design parameters, the constructed saturation compensator guarantees that, for all channels, the compensation signals  $\zeta_{i,1}(t)$  and  $\zeta_{i,2}(t)$  strictly converge to zero by  $t = T_\zeta$  or enter a prescribed arbitrarily small neighborhood; hence the compensator achieves uniform practical predefined-time stability at  $T_\zeta$ .

证明 Define the composite Lyapunov function

$$V_\zeta = \frac{1}{2} \sum_{i=1}^n (\zeta_{i,1}^2 + \zeta_{i,2}^2) = \sum_{i=1}^n W_i, \quad W_i = \frac{1}{2} (\zeta_{i,1}^2 + \zeta_{i,2}^2). \quad (62)$$

Taking the time derivative and using eq. (24) gives

$$\dot{V}_\zeta = \sum_{i=1}^n \left[ \zeta_{i,1} \delta_{i,1} + \zeta_{i,2} \delta_{i,2} - \mu_1 \zeta_{i,1}^2 - \mu_2 \zeta_{i,2}^2 + \zeta_{i,1} (\tilde{\alpha}_i - \alpha_i + \zeta_{i,2}) - g_i \zeta_{i,2} \Delta u_i \right], \quad (63)$$

For each channel  $i$ , by the power-mean inequality,  $|\zeta_{i,1}|^{2\pm\gamma} + |\zeta_{i,2}|^{2\pm\gamma} \geq (\zeta_{i,1}^2 + \zeta_{i,2}^2)^{1\pm\frac{\gamma}{2}} = (2W_i)^{1\pm\frac{\gamma}{2}}$ , which together with the predefined-time term yields

$$\zeta_{i,1} \delta_{i,1} + \zeta_{i,2} \delta_{i,2} \leq -\frac{\pi}{2\gamma T_\zeta} \left[ (2W_i)^{1-\frac{\gamma}{2}} + (2W_i)^{1+\frac{\gamma}{2}} \right] \leq -\frac{\pi}{2\gamma T_\zeta} \left[ W_i^{1-\frac{\gamma}{2}} + W_i^{1+\frac{\gamma}{2}} \right]. \quad (64)$$

By Young's inequality (Lemma 2), for any  $\mu_1, \mu_2 > 0$ ,

$$\zeta_{i,1} \zeta_{i,2} \leq \frac{1}{2} \zeta_{i,1}^2 + \frac{1}{2} \zeta_{i,2}^2, \quad (65a)$$

$$\zeta_{i,1} (\tilde{\alpha}_i - \alpha_i + \zeta_{i,2}) \leq \frac{\mu_1}{2} \zeta_{i,1}^2 + \frac{(\tilde{\alpha}_i - \alpha_i)^2}{2\mu_1}, \quad (65b)$$

$$|g_i \zeta_{i,2} \Delta u_i| \leq \frac{\mu_2}{2} \zeta_{i,2}^2 + \frac{g_i^2 (\Delta u_i)^2}{2\mu_2}. \quad (65c)$$

Substituting eqs. (64) and (65) into eq. (63), summing over  $i$ , and rearranging give

$$\dot{V}_\zeta \leq -\frac{\pi}{2\gamma T_\zeta} \sum_{i=1}^n \left( W_i^{1-\frac{\gamma}{2}} + W_i^{1+\frac{\gamma}{2}} \right) - \sum_{i=1}^n \left( \frac{1-\mu_1}{2} \zeta_{i,1}^2 + \frac{1-\mu_2}{2} \zeta_{i,2}^2 \right) + \sum_{i=1}^n \left( \frac{(\tilde{\alpha}_i - \alpha_i)^2}{2\mu_1} + \frac{g_i^2 (\Delta u_i)^2}{2\mu_2} \right). \quad (66)$$

Let

$$r_\zeta = \min_i \{1 - \mu_1, 1 - \mu_2\} > 0, \quad \Lambda = \sum_{i=1}^n \left( \frac{(\tilde{\alpha}_i - \alpha_i)^2}{2\mu_1} + \frac{g_i^2 (\Delta u_i)^2}{2\mu_2} \right),$$

Since  $\sum_{i=1}^n \left( \frac{1-\mu_1}{2} \zeta_{i,1}^2 + \frac{1-\mu_2}{2} \zeta_{i,2}^2 \right) \geq r_\zeta V_\zeta$ , discarding the stronger negative terms yields the linear comparison

$$\dot{V}_\zeta \leq -r_\zeta V_\zeta + \Lambda. \quad (67)$$

If the predefined-time terms are retained, then

$$\dot{V}_\zeta \leq -\frac{\pi}{2\gamma T_\zeta} \sum_{i=1}^n \left( W_i^{1-\frac{\gamma}{2}} + W_i^{1+\frac{\gamma}{2}} \right) + \Lambda. \quad (68)$$

If there exists  $\aleph > 0$  such that the trajectory enters and remains in  $\Xi = \{\zeta \in \mathbb{R}^{2n} : \|\zeta\| \leq \sqrt{\aleph}\}$ , then  $\Lambda$  is bounded and admits the explicit bound

$$\Lambda \leq \Lambda(\aleph) = \sum_{i=1}^n \left( \frac{\sup_{t \geq 0} (\tilde{\alpha}_i - \alpha_i)^2}{2\mu_1} + \frac{g_i^2 \sup_{t \geq 0} (\Delta u_i)^2}{2\mu_2} \right) < \infty. \quad (69)$$

Applying Lemma 1 at  $t = T_\zeta$ ,

$$V_\zeta(T_\zeta) \leq \min \left\{ \left( \frac{2\gamma T_\zeta \Lambda}{\pi} \right)^{\frac{1}{1-\frac{\gamma}{2}}}, \left( \frac{2\gamma T_\zeta \Lambda}{\pi} \right)^{\frac{1}{1+\frac{\gamma}{2}}} \right\}. \quad (70)$$

When  $(\tilde{\alpha}_i - \alpha_i) = 0$  and  $\Delta u_i = 0$ , one has  $\Lambda = 0$ , and eq. (68) implies convergence to the origin by  $T_\zeta$ ; otherwise the trajectory enters the above arbitrarily small neighborhood by  $T_\zeta$  and remains therein. This completes the proof.  $\square$

## 6 Simulation and Experiment

### 6.1 Simulation

we consider the 2-DOF manipulator, where  $x_1 = [q_1, q_2]^\top$  represents the joint angles of the manipulator. The dynamic model is as follows, the inertia matrix  $M_0(q)$ :  $M_{11} = r_1 + r_2 + 2r_3 \cos q_2$ ,  $M_{12} = M_{21} = r_2 + r_3 \cos q_2$ ,  $M_{22} = r_2$ ; the centrifugal matrix  $C_0(q, \dot{q})$ :  $C_{11} = -r_3 \dot{q}_2 \sin q_2$ ,  $C_{12} = -r_3 (\dot{q}_1 + \dot{q}_2) \sin q_2$ ,  $C_{21} = r_3 \dot{q}_1 \sin q_2$ ,  $C_{22} = 0$ ; The gravity vector  $G_0(q)$ :  $G_1 = r_4 g \cos q_1 + r_5 g \cos(q_1 + q_2)$ ,  $G_2 = r_5 g \cos(q_1 + q_2)$ .

The lumped constants are  $r_1 = m_1 l_{c1}^2 + I_1 + m_2 l_1^2$ ,  $r_2 = I_2 + m_2 l_{c2}^2$ ,  $r_3 = m_2 l_1 l_{c2}$ ,  $r_4 = m_1 l_{c1} + m_2 l_1$ ,  $r_5 = m_2 l_{c2}$ . Here,  $m_i$ ,  $I_i$ , and  $l_i$  are the mass, moment of inertia, and length of the  $i$ th link, respectively, and  $l_{ci}$  is the distance from the  $(i-1)$  joint to the center of mass of the  $i$ th link; The mass and inertia parameters are set as:  $m_1 = 1$  kg,  $m_2 = 3$  kg,  $l_1 = 0.31$  m,  $l_2 = 0.35$  m,  $l_{c1} = 0.15$  m,  $l_{c2} = 0.18$  m,  $I_1 = 0.1$  kg m<sup>2</sup>,  $I_2 = 0.02$  kg m<sup>2</sup>,  $g = 9.8$  m/s<sup>2</sup>.

The control objective is to design the control torque  $u$  so that the joints track a desired joint-space trajectory within prescribed performance and a predefined-time. The initial velocity is  $\dot{x}(0) = [\dot{q}_1(0), \dot{q}_2(0)]^\top = [0, 0]^\top$  rad/s. The desired joint trajectories are  $q_d = [0.1 \sin(0.5t) + \cos(0.5t), 0.1 \sin(t) + \cos(t)]^\top$ ,  $\dot{q}_d = [0.05 \cos(0.5t) - 0.5 \sin(0.5t), 0.1 \cos(t) - \sin(t)]^\top$ . With  $\nu_0 = 1$ ,  $\nu_1 = 1$ ,  $\nu_2 = 0$ ,  $\nu_3 = 0$ , then the prescribed performance function for each joint is  $\rho_i(t) = \rho_i(\infty) + (\rho_i(0) - \rho_i(\infty)) [1 - 4(t/T_p)^{3p} + 3(t/T_p)^{4p}]$ , and its parameters are set as  $p = 0.3$ ,  $\rho_1(0) = 2$ ,  $\rho_1(\infty) = 0.02$ ,  $\rho_2(0) = 4$ ,  $\rho_2(\infty) = 0.01$ ,  $v_1 = 6$ ,  $v_2 = 4$ , and the predefined-time  $T_p$  is user-defined according to the simulation requirements. The controller parameters are set as:  $c = 0.6$ ,  $\gamma = 0.4$ ,  $\alpha \in [-40, 40]$ ,  $\lambda = 5$ ,  $\omega \in [0.5, 2]$ ,  $\vartheta = 0.1$ ,  $v_1 = 8$ ,  $v_2 = 8$ ,  $\hbar_1 = \hbar_2 = 6$ ,  $\varpi_1 = \varpi_2 = 8$ ,  $\eta = 0.1$ ,  $k_1 = \text{diag}(42, 42)$ ,  $k_2 = \text{diag}(6, 6)$ . The controller's step size is  $h = 0.001$ . The input torque is saturated as  $u \in [-10, 10]$  N·m. The parameters of RBFNN are set as  $N = 5$ ,  $o \in \mathbb{R}^{(2n) \times N}$  are sampled uniformly in  $[-1, 1]$ ,  $D \in \mathbb{R}^N$  with  $D_i = 2$  for  $i = 1, \dots, N$ ,  $\beta = [20, 20]$ ,  $\varrho = [10, 10]$ .

#### Case 1: Different convergence times

To further verify the time-constrained stability of the proposed control method, we conduct a series of simulations to examine the impact of the predefined-time  $T_p$  on system performance. We select  $T_p \in \{1.5, 2.5, 3.5\}$  s while fixing the initial state at  $x_1(0) = [\pi/2, \pi/2]^\top$ ; all other parameters are kept unchanged. The results in figs. 2 to 4 show that in all cases the error enters the prescribed envelope before  $T_p$  and converges to zero, confirming strict tunability with respect to  $T_p$ . With  $T_p = 1.5$  s, the torques saturate early but the anti-saturation compensation maintains convergence. With  $T_p = 3.5$  s, the decay is slower and mild high-frequency ripple appears, yet constraints and stability are preserved, indicating fast corrective action by the compensator. Overall, the controller achieves the desired timing and accuracy across  $T_p$  settings, even under input saturation.

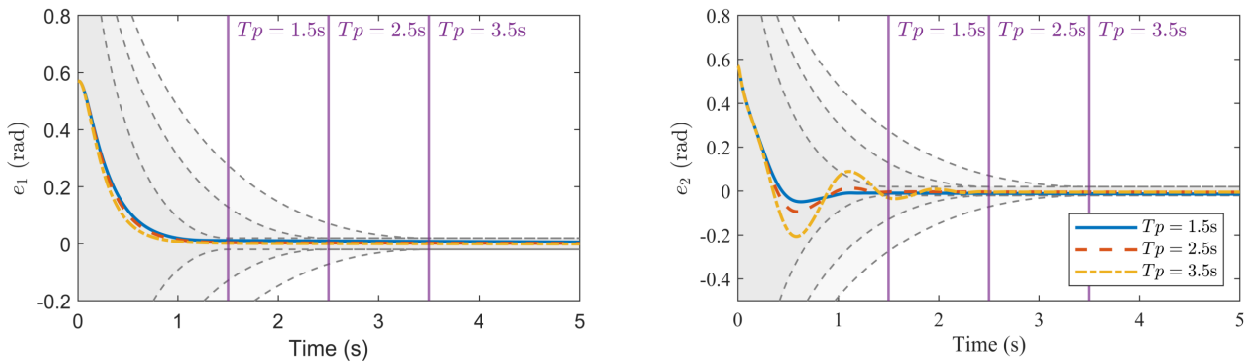


图 2 Position tracking errors under different predefined times  $T_p$ .

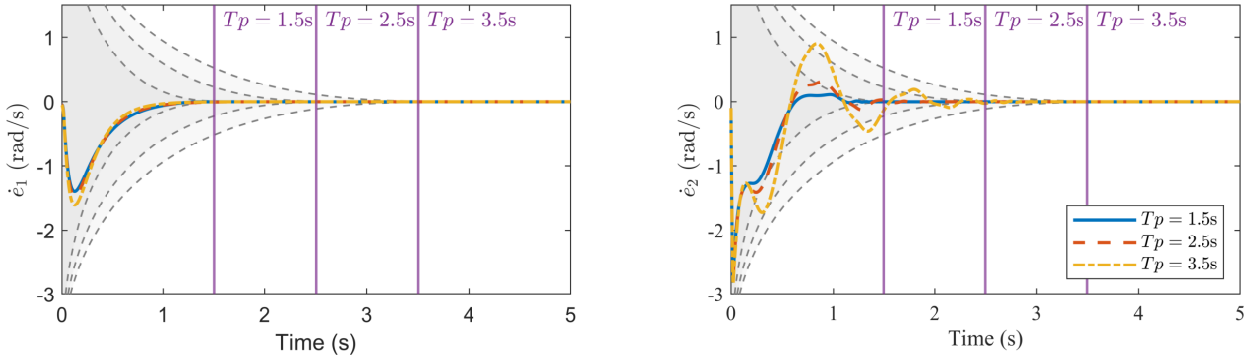


图 3 Velocity tracking errors under different predefined times  $T_p$ .

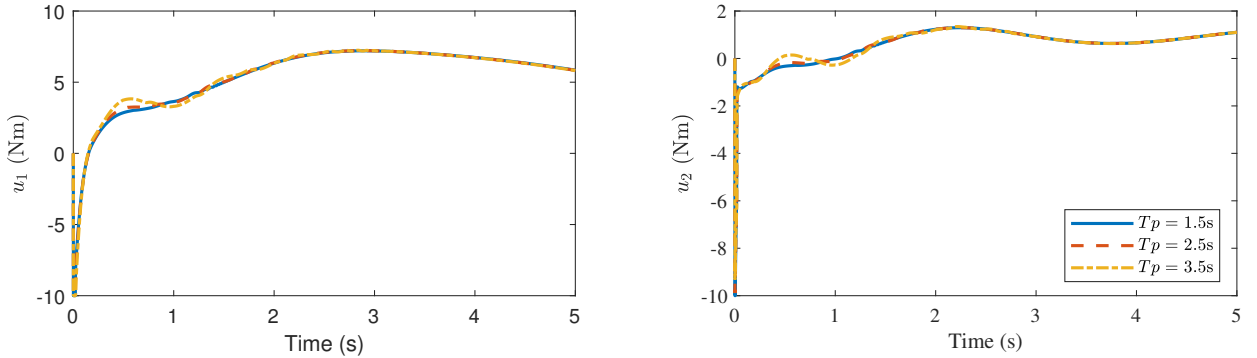


图 4 Control input torques under different predefined times  $T_p$ .

## Case 2: Different initial state conditions

To assess how initial states affect control performance under input saturation and its compensation, we fix the predefined-time at  $T_p = 2.5\text{s}$  and test two classes of initial conditions: in-envelope  $x_1(0) \in \{[\pi/2, \pi/2]^\top, [\pi/4, \pi/4]^\top, [0, \pi/2]^\top\}$  and out-of-envelope  $x_1(0) \in \{[\pi, \pi]^\top, [-\pi/2, -\pi/2]^\top, [-3\pi/4, -3\pi/4]^\top\}$ . The results in figs. 5 to 7 show that, for in-envelope cases, the system achieves fast and smooth tracking: errors decay to near zero before  $T_p$ , velocity responses exhibit no noticeable ripple, and torque magnitudes remain moderate. For out-of-envelope cases, errors enter the prescribed envelope within  $0.5 - 1.5\text{s}$  and still converge by  $T_p$ ; torques are larger early on but drop quickly, indicating strong initial drive followed by stabilization. These findings confirm that, with input saturation and anti-saturation compensation, the proposed controller ensures error “legalization” (entry into the envelope) and global convergence within  $T_p$  regardless of the initial condition, i.e., the time of convergence is independent of the initial state.

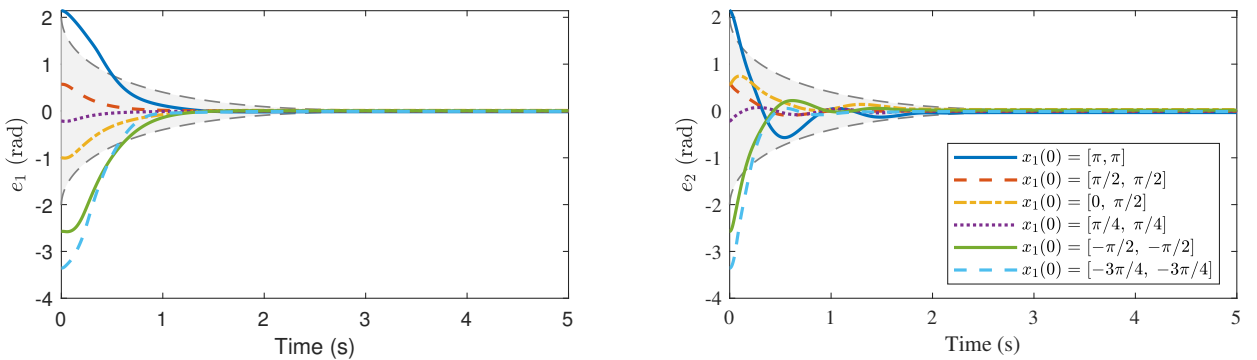


图 5 Position tracking errors under different initial values of  $x_1(0)$ .

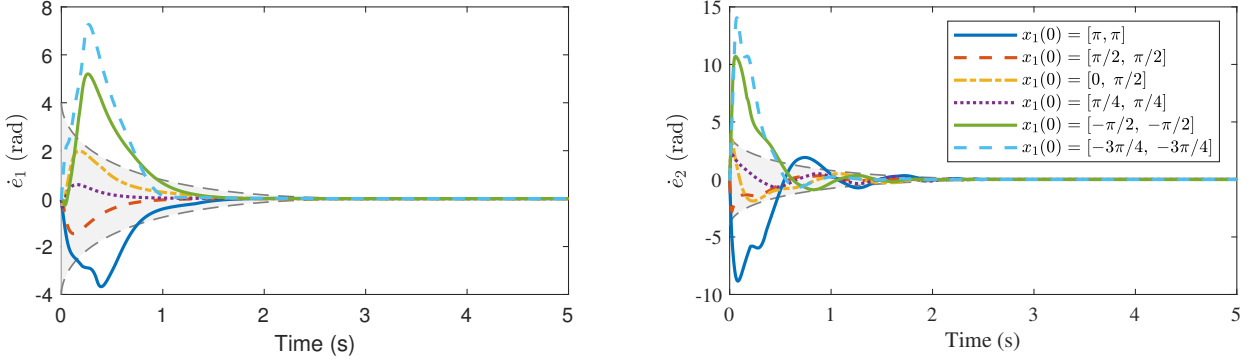


图 6 Velocity tracking errors under different initial values of  $x_1(0)$ .

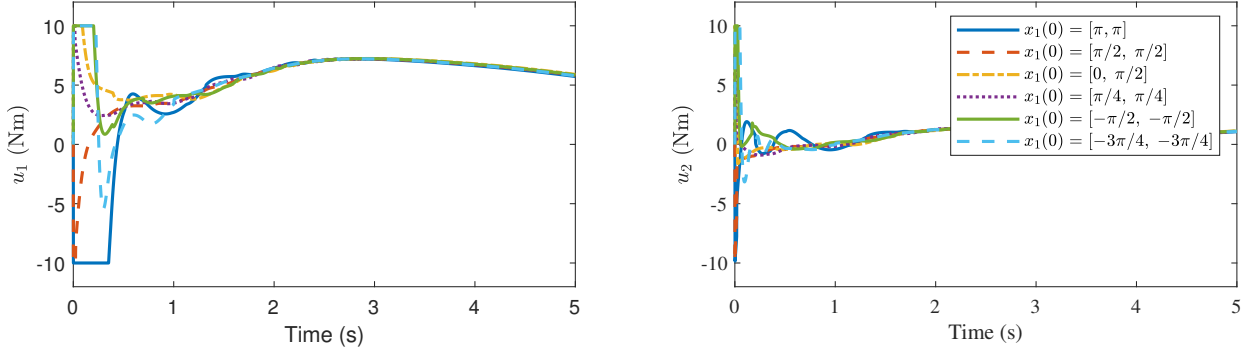


图 7 Control input torques under different initial value of  $x_1(0)$ .

### Case 3: Comparison of algorithms

To comprehensively evaluate the proposed method, we compare four representative controllers: predefined-time control without performance constraints (PTC), prescribed-performance asymptotic stability control (PPC), fixed-time control (FTC, see [12]), and predefined-time control with prescribed-performance constraints (PTPPC). Our method (Proposed) combines a displacement-based performance shaping function, predefined-time regulation, and anti-saturation compensation. We fix  $T_p = 2.5$  s and test two initial conditions:  $x_1(0) = [\pi/2, \pi/2]^\top$  (in-envelope error, figs. 8 to 10) and  $x_1(0) = [-\pi/2, -\pi/2]^\top$  (out-of-envelope error, figs. 11 to 13).

For the in-envelope error case (figs. 8 to 10), PPC yields smooth steady-state behavior but slow convergence; FTC converges faster yet shows irregular jumps and rebounds; PTC meets the time target but exhibits large initial fluctuations. PTPPC compresses the error within the prescribed bounds by  $T_p$  with relatively smooth inputs. Building on this, the Proposed controller—via the error-shift function and anti-saturation compensation—keeps the error within the envelope throughout, achieves faster convergence, smoother actuation, and lower actuator effort, with no noticeable torque overshoot or chattering.

For the out-of-envelope error case (figs. 11 to 13), differences are amplified. PTC and FTC display pronounced oscillations and short-term divergence; FTC often drives torques to their limits for extended periods. PPC and PTPPC lack rapid correction for out-of-envelope initial errors, leaving the error outside the bounds and producing highly oscillatory inputs with limited regulation. In contrast, the Proposed method still legalizes the error and ensures stable convergence by  $T_p$ , with bounded and smooth inputs, demonstrating strong robustness and superior overall performance.

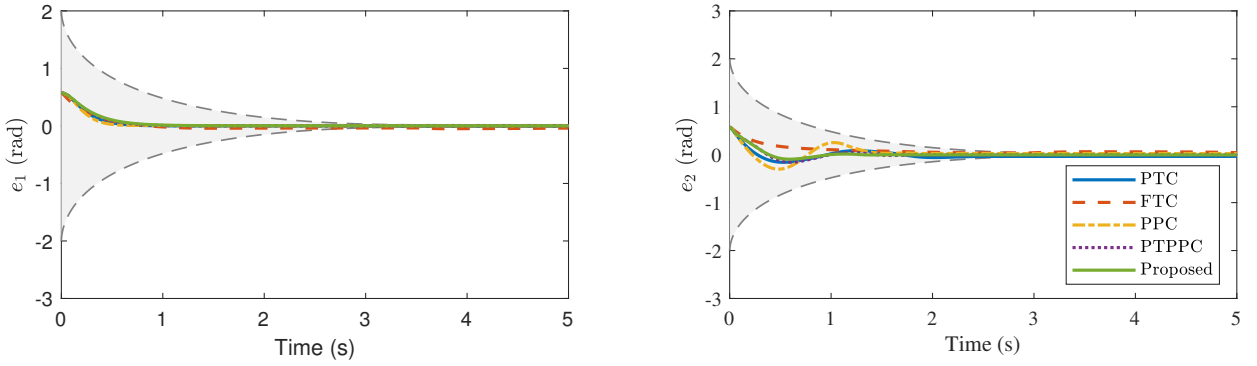


图 8 Comparison of position tracking errors under different methods with in-bound initial errors.

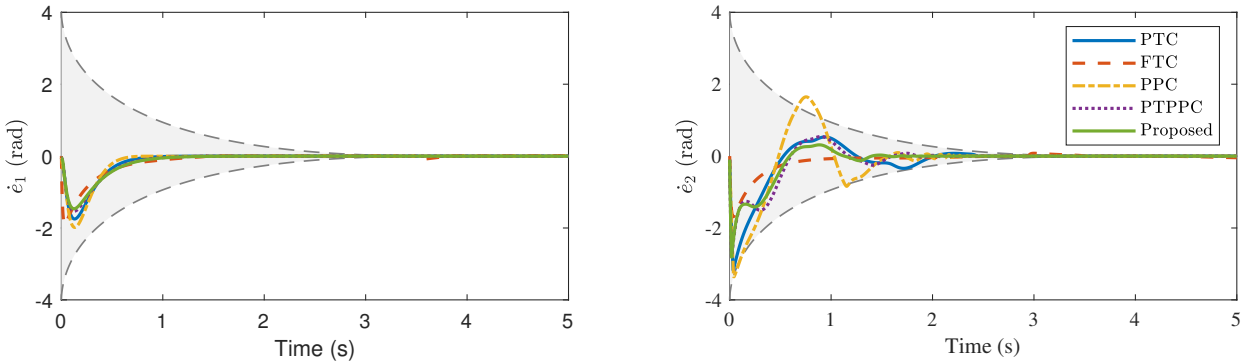


图 9 Comparison of velocity tracking errors under different methods with in-bound initial errors.

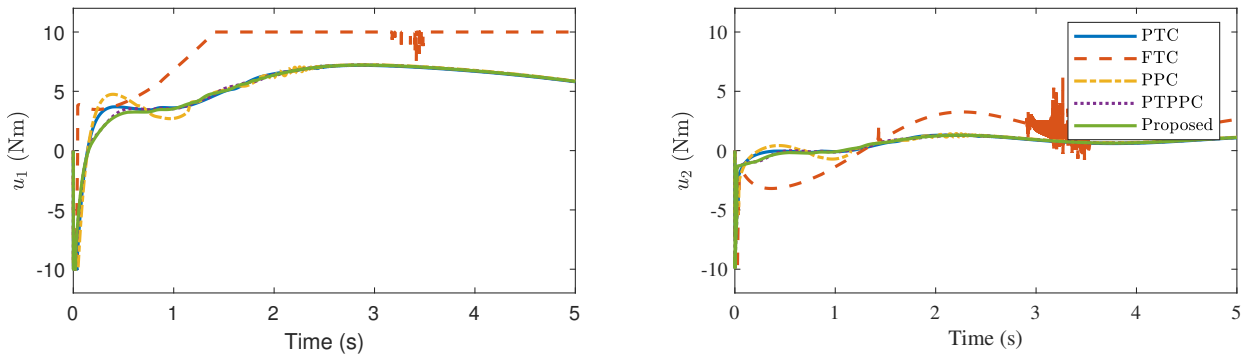


图 10 Comparison of control input torques under different Methods with in-bound initial errors.

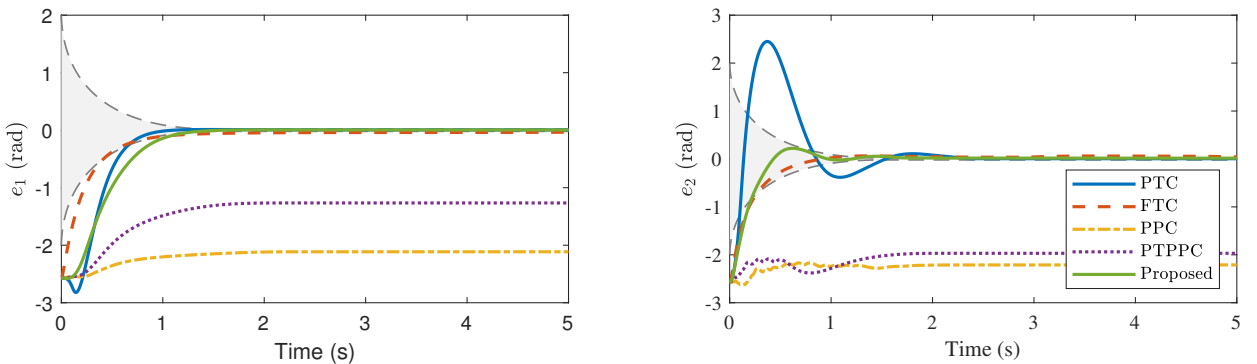


图 11 Comparison of position tracking errors under different methods with out-of-bound initial errors.

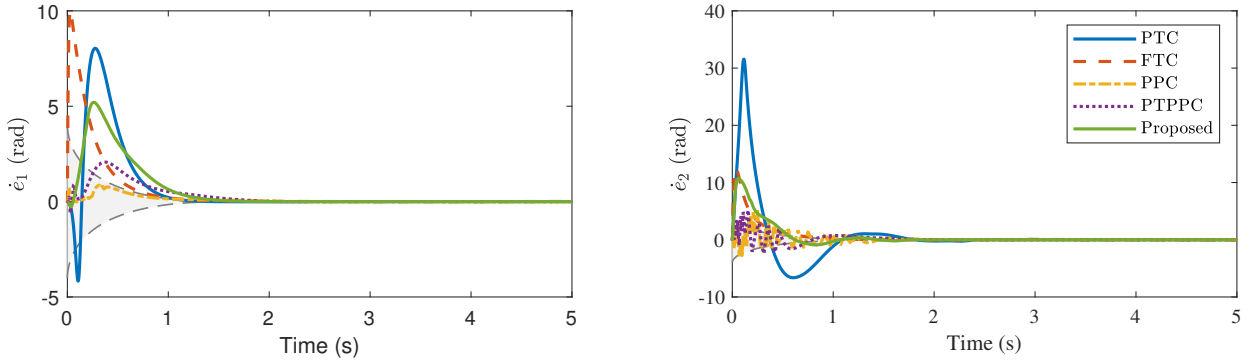


图 12 Comparison of velocity tracking errors under different methods with out-of-bound initial errors.

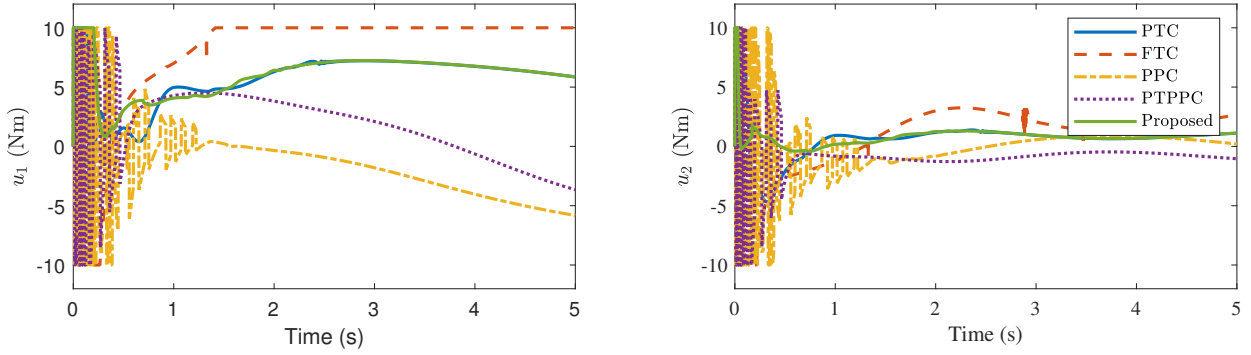


图 13 Comparison of control input torques under different Methods with out-of-bound initial errors.

## 6.2 Experiment

To further validate the effectiveness of the proposed method in real high DOF industrial robotic systems. A 6-DOF collaborative manipulator of JAKA C7 as shown in fig. 14 is selected as the controlled object to carry out the trajectory tracking simulation experiments of six joints. The control objective is to enable each joint to track accurately along a set reference trajectory, while ensuring that all tracking errors converge within a specified predefined-time and always satisfy the given performance boundary constraints.

The parameters of prescribed performance function are set as  $p = 0.6, \rho_1(0) = \pi/2, \rho_1(\infty) = 0.02, \rho_2(0) = \pi, \rho_2(\infty) = 0.02$ . The predefined convergence time is set  $T_p = 3$  s. The controller parameters are set as:  $c = 0.6, \gamma = 0.4, \alpha_{\min} = -100, \alpha_{\max} = 100, \lambda = 2.5, \omega_{\min} = 2, \omega_{\max} = 6$ , The control input is  $u_{\min} = -u_{\max}, u_{\max} = [60; 60; 40; 30; 20; 15], k_1 = \text{diag}(30, 30, 30, 24, 24, 30), k_2 = \text{diag}(12, 10, 12, 10, 8, 8)$ . The remaining parameters are set consistent with those in the simulation subsection. The desired joint trajectories are constructed to cover a range of frequency components and are defined as follows  $q_d(t) = [0.1 \sin(0.5t) + \cos(0.5t), 0.1 \sin(t) + \cos(t), 0.2 \sin(1.5t) + 0.8 \cos(t), 0.3 \sin(2t) + 0.7 \cos(0.5t), 0.1 \sin(0.3t) + 0.9 \cos(0.2t), 0.4 \sin(t) + 0.6 \cos(2t)]$ .

To validate the effectiveness of the proposed control method, we conduct comparative simulations on a representative 6-DOF manipulator model with four controllers: predefined-time control without performance constraints (PTC), prescribed-performance asymptotic stability control (PPC), predefined-time control with prescribed-performance constraints (PTPPC), and the proposed controller (Proposed). We fix the predefined-time at  $T_p = 3$  s and specify jointwise performance envelopes  $\rho_i(t)$ . The initial values of the the manipulator are  $x(0) = [\pi/2, -\pi/2, \pi/3, -\pi/3, \pi/2, -\pi/2]$  rad,  $\dot{x}(0) = \mathbf{0}$  rad/s. Importantly, the initial errors of joints 2, 4, and 6 exceed their respective bounds, whereas joints 1, 3, and 5 start within the envelopes, yielding two distinct dynamics: (i) for joints 2/4/6, the controller must first drive the errors back inside the bounds before tracking; (ii) for joints 1/3/5, the errors decay directly under the prescribed performance. The transient responses across algorithms are presented side by side in figs. 15 to 19.

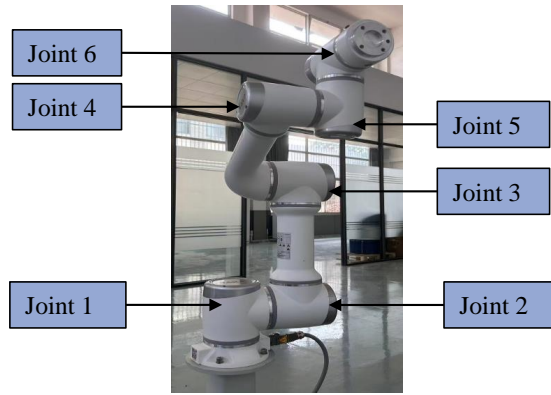


图 14 The 6-DOF collaborative manipulator of JAKA C7.

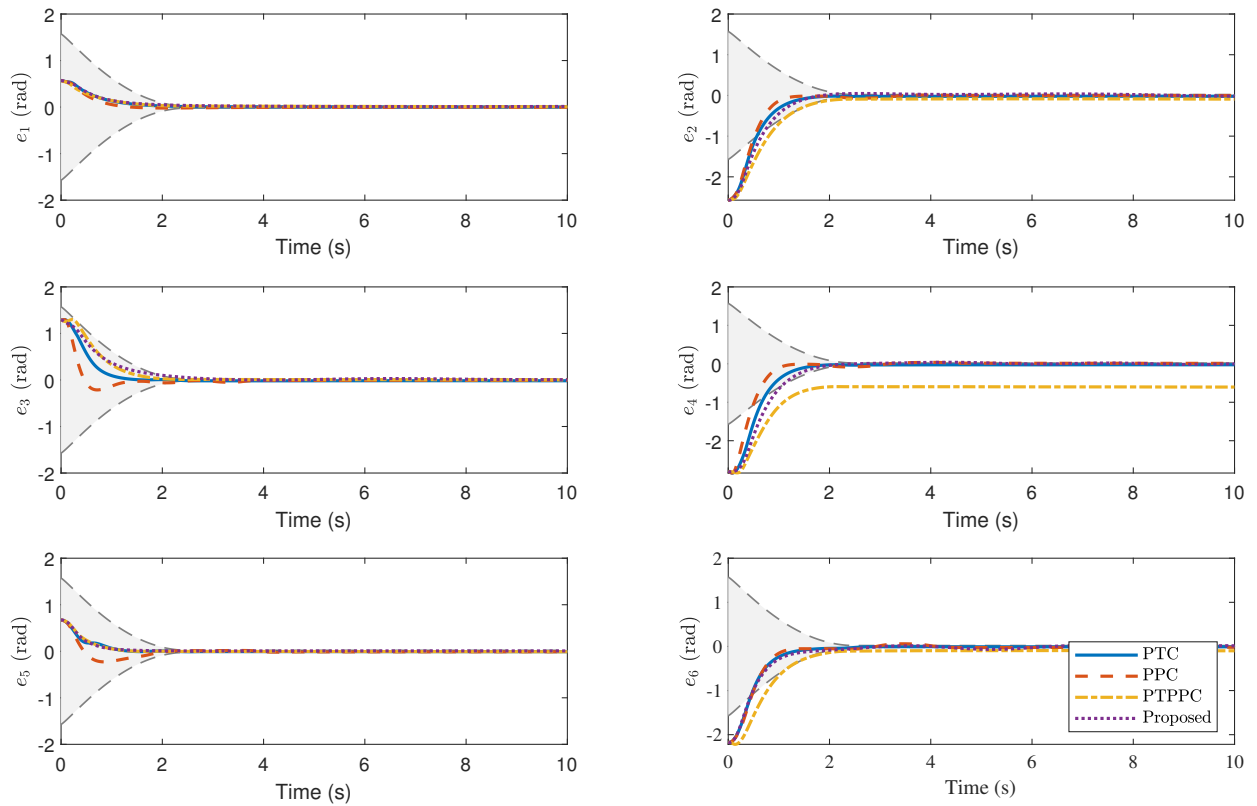


图 15 Comparison of position tracking errors under different methods of 6-DOF manipulator.

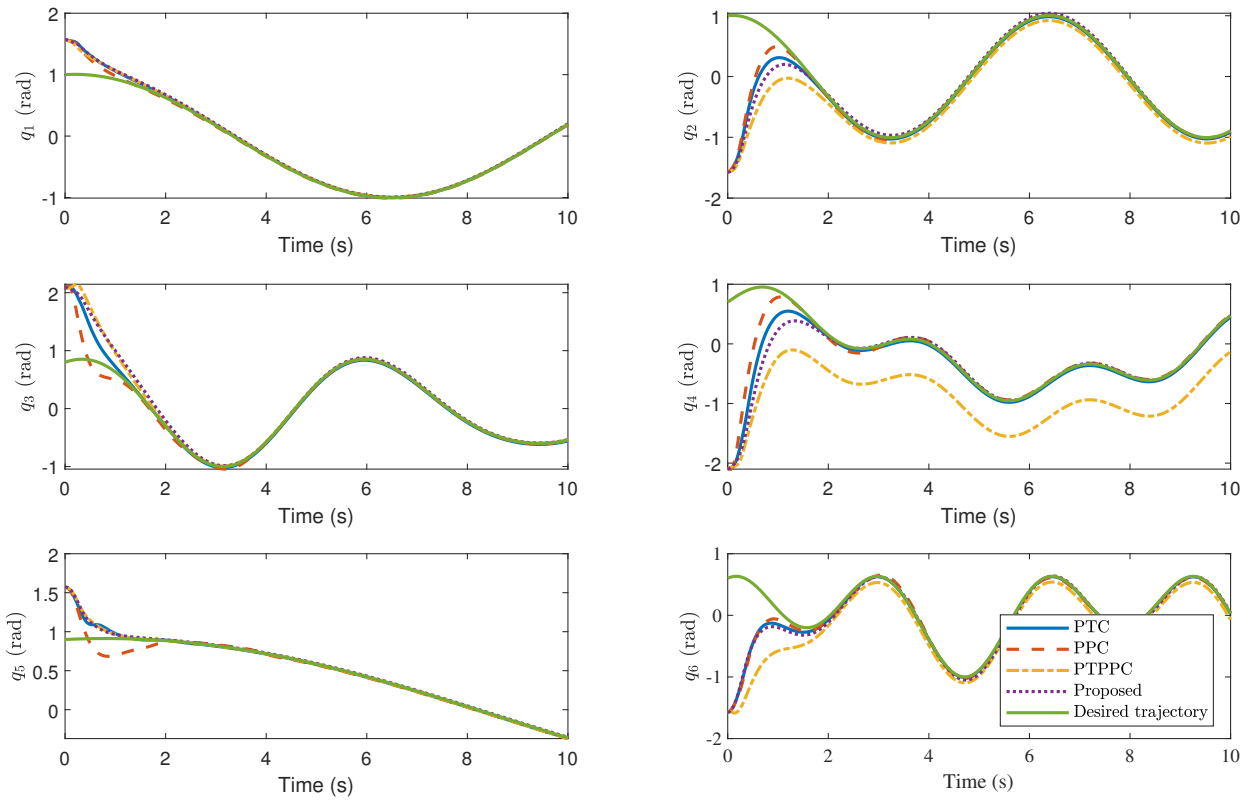


图 16 Comparison of position tracking trajectories under different methods of 6-DOF manipulator.

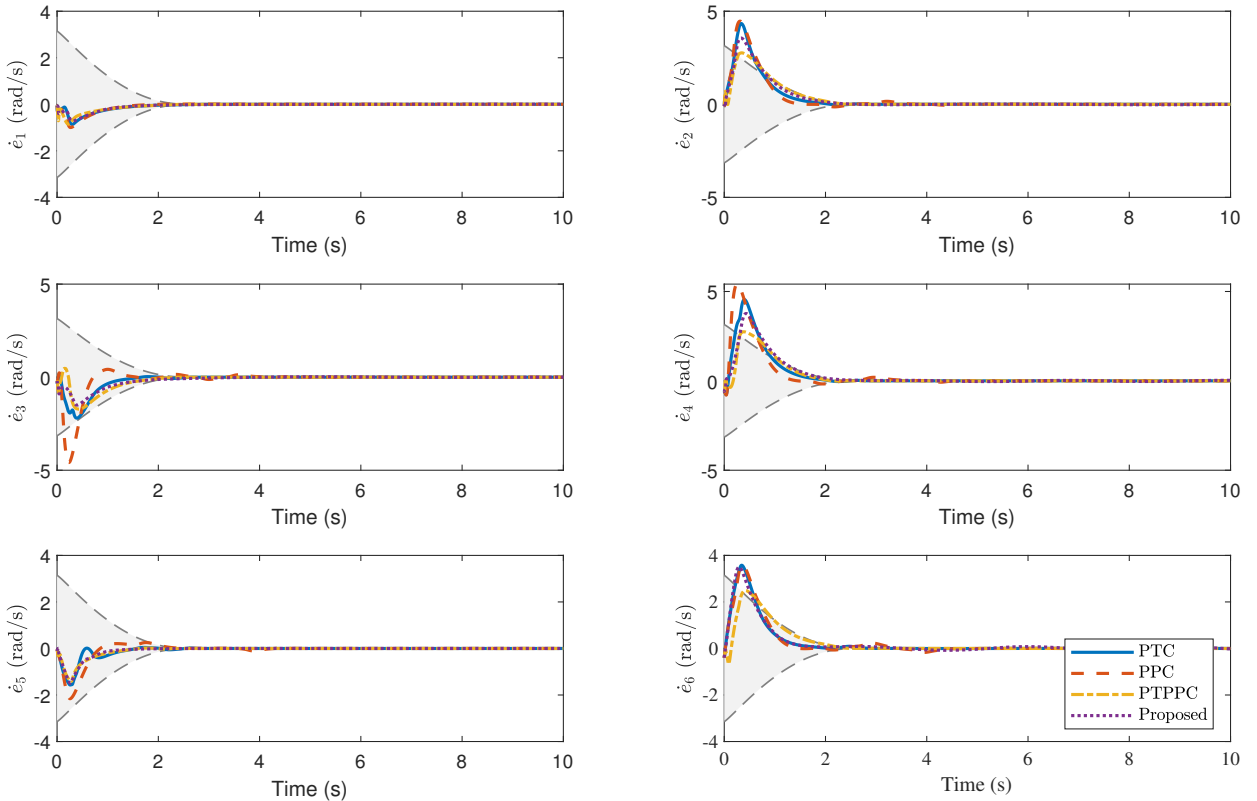


图 17 Comparison of velocity tracking errors under different methods of 6-DOF manipulator.

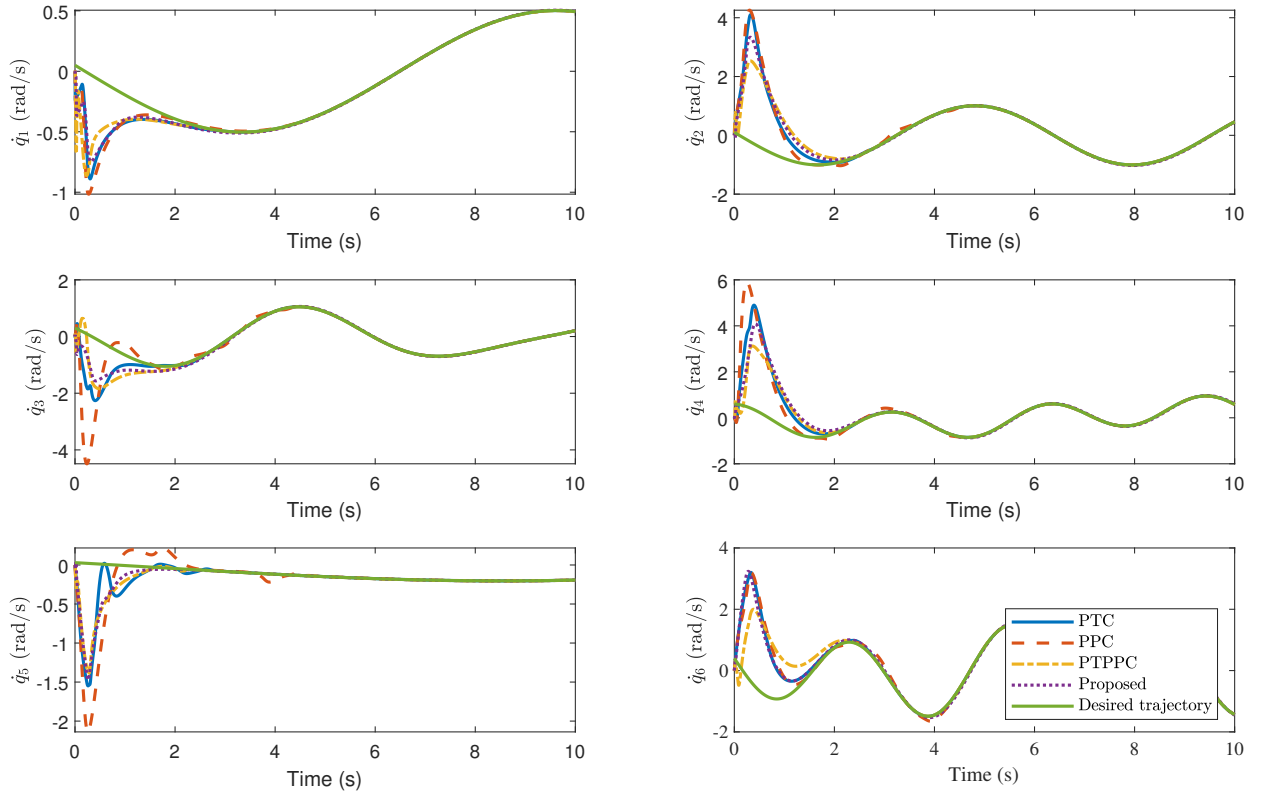


图 18 比较不同方法下 6-DOF 机器人速度跟踪性能。

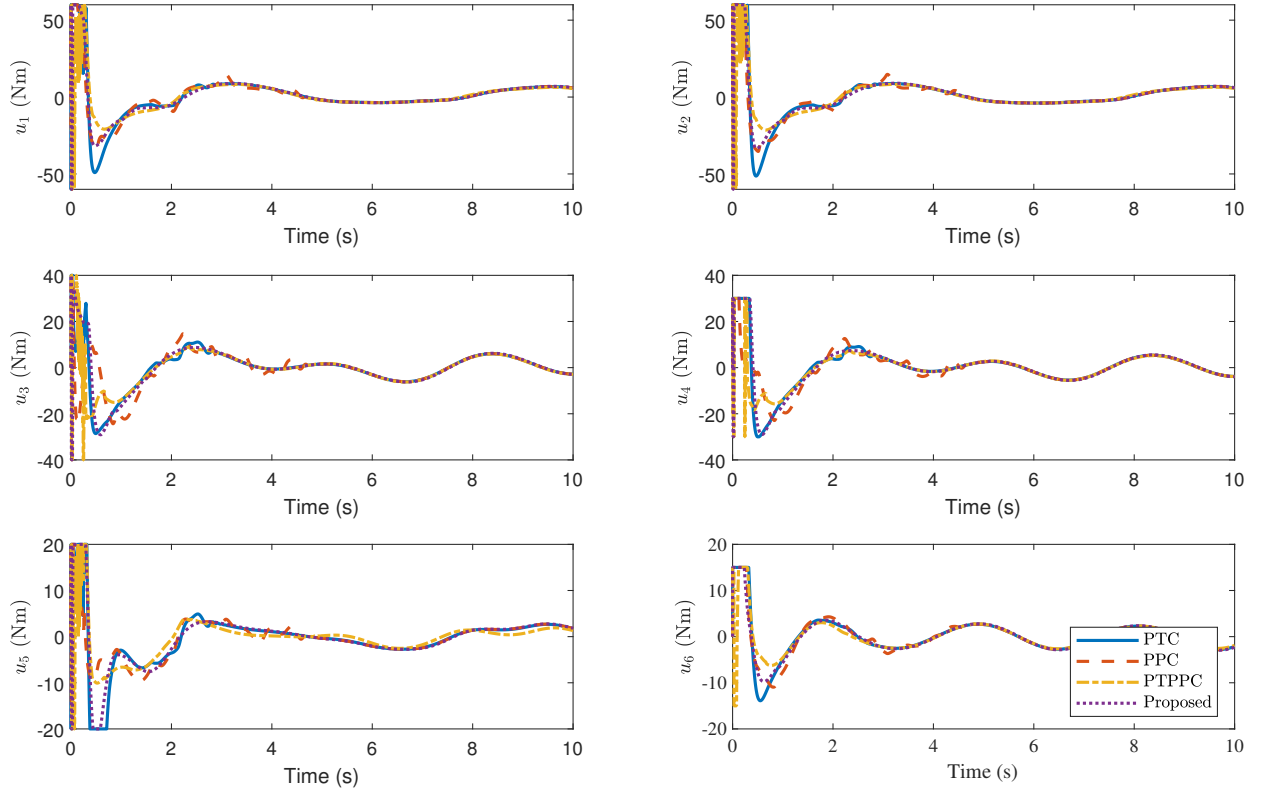


图 19 比较不同方法下 6-DOF 机器人控制输入扭矩。

As shown in figs. 15 to 19, after a comprehensive comparison of the four controllers, both PTC and the Proposed method achieve convergence within  $T_p = 3$ s. However, thanks to the added displacement-function modulation and anti-saturation compensation, the Proposed method shows virtually no overshoot and much smoother torques, yielding clearly superior transient and steady-state quality to PTC. PPC complies with the

prescribed-performance framework but, lacking explicit time enforcement and saturation handling, exhibits large oscillations in position/velocity errors during 0–2 s, converges the slowest, and still leaves residual error after 3 s, thus failing the time requirement. PTPPC responds poorly to large out-of-envelope initial errors; in particular, the errors of joints 2, 4, and 6 remain outside the bounds and the legalization step is not completed. Overall, the Proposed controller surpasses PTC, PPC, and PTPPC in convergence speed, steady-state accuracy, chattering suppression, and actuator load. The coordinated design enforces the time–performance dual constraints and, via saturation compensation, reduces energy consumption and thermal load, making it suitable for high-DOF manipulators with large initial deviations under input limits.

## 7 Conclusion

This work proposes an adaptive backstepping controller that combines predefined-time convergence and global prescribed-performance constraints. The goal is trajectory tracking for manipulators with unknown dynamics, bounded disturbances, and input saturation. We design a channel-wise predefined-time error transformation. It removes initial-condition singularities and nonsmooth mappings in conventional PPC. It enforces strict, smooth, global bounds regardless of the initial state. We also add a unified auxiliary compensator. It quickly cancels saturation residuals between virtual and actual inputs and curbs computational growth. A first-order sliding-mode observer and an RBFNN estimator handle disturbances and unmodeled dynamics. Lyapunov analysis proves predefined-time stability and error convergence. Simulations and hardware experiments show clear gains over baselines. The method legalizes large initial errors fast, meets performance within the prescribed time, and reduces actuator torque. Future work will test on real robots under tougher conditions such as parameter drift, delays, abrupt disturbances, and task switching. We will also explore safe integration with learning-based methods with provable convergence for high-DOF, multi-task systems.

## References

- [1] Sciavicco, L., Siciliano, B.: Modelling and Control of Robot Manipulators. Springer, London (2012). <https://doi.org/10.1007/978-1-4471-0449-0>
- [2] Bagheri, M., Naseradinmousavi, P., Krstić, M.: Feedback linearization based predictor for time delay control of a high-dof robot manipulator. *Automatica* **108**, 108485 (2019-10) <https://doi.org/10.1016/j.automatica.2019.06.037>
- [3] Spong, M.W.: An historical perspective on the control of robotic manipulators. *Annual Review of Control, Robotics, and Autonomous Systems* **5**(1), 1–31 (2022-05-03) <https://doi.org/10.1146/annurev-control-042920-094829>
- [4] Shojaei, K., Kazemy, A., Chatraei, A.: An observer-based neural adaptive \$pid^2\$ controller for robot manipulators including motor dynamics with a prescribed performance. *IEEE/ASME Transactions on Mechatronics* **26**(3), 1689–1699 (2021-06) <https://doi.org/10.1109/TMECH.2020.3028968>
- [5] Zhou, B., Yang, L., Wang, C., Lai, G., Chen, Y.: Adaptive finite-time tracking control of robot manipulators with multiple uncertainties based on a low-cost neural approximator. *Journal of the Franklin Institute* **359**(10), 4938–4958 (2022-07) <https://doi.org/10.1016/j.jfranklin.2022.04.025>
- [6] Xu, S., He, B.: Robust adaptive fuzzy fault tolerant control of robot manipulators with unknown parameters. *IEEE Transactions on Fuzzy Systems* **31**(9), 3081–3092 (2023-09) <https://doi.org/10.1109/TFUZZ.2023.3244189>

- [7] Wang, M., Yang, A.: Dynamic learning from adaptive neural control of robot manipulators with prescribed performance. *IEEE Transactions on Systems, Man, and Cybernetics: Systems* **47**(8), 2244–2255 (2017-08) <https://doi.org/10.1109/TSMC.2016.2645942>
- [8] Zhang, D., Hu, J., Cheng, J., Wu, Z.-G., Yan, H.: A novel disturbance observer based fixed-time sliding mode control for robotic manipulators with global fast convergence. *IEEE/CAA Journal of Automatica Sinica* **11**(3), 661–672 (2024-03) <https://doi.org/10.1109/JAS.2023.123948>
- [9] Yang, P., Su, Y.: Proximate fixed-time prescribed performance tracking control of uncertain robot manipulators. *IEEE/ASME Transactions on Mechatronics* **27**(5), 3275–3285 (2022-10) <https://doi.org/10.1109/TMECH.2021.3107150>
- [10] Zhai, J., Li, Z.: Fast-exponential sliding mode control of robotic manipulator with super-twisting method. *IEEE Transactions on Circuits and Systems II: Express Briefs* **69**(2), 489–493 (2022-02) <https://doi.org/10.1109/TCSII.2021.3081147>
- [11] Incremona, G.P., Ferrara, A., Magni, L.: Mpc for robot manipulators with integral sliding modes generation. *IEEE/ASME Transactions on Mechatronics* **22**(3), 1299–1307 (2017-06) <https://doi.org/10.1109/TMECH.2017.2674701>
- [12] Cao, S., Sun, L., Jiang, J., Zuo, Z.: Reinforcement learning-based fixed-time trajectory tracking control for uncertain robotic manipulators with input saturation. *IEEE Transactions on Neural Networks and Learning Systems* **34**(8), 4584–4595 (2023-08) <https://doi.org/10.1109/TNNLS.2021.3116713>
- [13] Wu, J., Chen, S., Wang, Y., Zhang, P., Su, C.-Y., Sato, D.: A transfer reinforcement learning-based control method for vertical n-link underactuated manipulator with two passive joints. *IEEE/ASME Transactions on Mechatronics*, 1–10 (2024) <https://doi.org/10.1109/TMECH.2024.3419803>
- [14] Liu, Y., Liu, X., Jing, Y.: Adaptive neural networks finite-time tracking control for non-strict feedback systems via prescribed performance. *Information Sciences* **468**, 29–46 (2018-11) <https://doi.org/10.1016/j.ins.2018.08.029>
- [15] Liu, C., Zhao, K., Li, J., Yang, C.: Fuzzy adaptive predefined time control with global prescribed performance for robotic manipulator under unknown disturbance. *IEEE Transactions on Systems, Man, and Cybernetics: Systems*, 1–14 (2025) <https://doi.org/10.1109/TSMC.2025.3540777>
- [16] Wang, L., Qi, R., Jiang, B.: Adaptive actuator fault-tolerant control for non-minimum phase air-breathing hypersonic vehicle model. *ISA Transactions* **126**, 47–64 (2022) <https://doi.org/10.1016/j.isatra.2021.07.032>
- [17] Bacciotti, A., Rosier, L.: *Liapunov Functions and Stability in Control Theory*. Communications and Control Engineering. Springer, Berlin, Heidelberg (2005). <https://doi.org/10.1007/b139028>
- [18] Song, Z., Li, P.: General lyapunov stability and its application to time-varying convex optimization. *IEEE/CAA Journal of Automatica Sinica* **11**(11), 2316–2326 (2024-11) <https://doi.org/10.1109/JAS.2024.124374>
- [19] Liu, Y., Li, H., Lu, R., Zuo, Z., Li, X.: An overview of finite/fixed-time control and its application in engineering systems. *IEEE/CAA Journal of Automatica Sinica* **9**(12), 2106–2120 (2022-12) <https://doi.org/10.1109/JAS.2022.105413>
- [20] Song, X., Sun, P., Song, S., Stojanovic, V.: Finite-time adaptive neural resilient dsc for fractional-order

- nonlinear large-scale systems against sensor-actuator faults. *Nonlinear Dynamics* **111**(13), 12181–12196 (2023-07) <https://doi.org/10.1007/s11071-023-08456-0>
- [21] Polyakov, A.: Nonlinear feedback design for fixed-time stabilization of linear control systems. *IEEE Transactions on Automatic Control* **57**(8), 2106–2110 (2012-08) <https://doi.org/10.1109/TAC.2011.2179869>
- [22] Zhang, Y., Pang, K., Hua, C.: Global composite learning fixed-time control of robotic systems with asymmetric tracking error constraints. *IEEE Transactions on Industrial Electronics* **70**(7), 7082–7091 (2023-07) <https://doi.org/10.1109/TIE.2022.3206694>
- [23] Guo, W., Wang, L., Shi, L., Sun, W., Jahanshahi, H.: Predefined-time stability for a class of dynamical systems and its application on the consensus control for nonlinear multi-agent systems. *Information Sciences* **626**, 180–203 (2023-05) <https://doi.org/10.1016/j.ins.2023.01.063>
- [24] Fan, Y., Zhan, H., Li, Y., Yang, C.: A predefined time constrained adaptive fuzzy control method with singularity-free switching for uncertain robots. *IEEE Transactions on Fuzzy Systems* **32**(5), 2650–2662 (2024-05) <https://doi.org/10.1109/TFUZZ.2024.3357124>
- [25] Wang, Q., Cao, J., Liu, H.: Adaptive fuzzy control of nonlinear systems with predefined time and accuracy. *IEEE Transactions on Fuzzy Systems* **30**(12), 5152–5165 (2022-12) <https://doi.org/10.1109/TFUZZ.2022.3169852>
- [26] Sun, Y., Gao, Y., Zhao, Y., Liu, Z., Wang, J., Kuang, J., Yan, F., Liu, J.: Neural network-based tracking control of uncertain robotic systems: Predefined-time nonsingular terminal sliding-mode approach. *IEEE Transactions on Industrial Electronics* **69**(10), 10510–10520 (2022-10) <https://doi.org/10.1109/TIE.2022.3161810>
- [27] Li, L., Liu, Z., Guo, S., Ma, Z., Huang, P.: Adaptive practical predefined-time control for uncertain teleoperation systems with input saturation and output error constraints. *IEEE Transactions on Industrial Electronics* **71**(2), 1842–1852 (2024-02) <https://doi.org/10.1109/TIE.2023.3250752>
- [28] Shen, H., Zhao, W., Cao, J., Park, J.H., Wang, J.: Predefined-time event-triggered tracking control for nonlinear servo systems: A fuzzy weight-based reinforcement learning scheme. *IEEE Transactions on Fuzzy Systems* **32**(8), 4557–4569 (2024-08) <https://doi.org/10.1109/TFUZZ.2024.3403917>
- [29] Bechlioulis, C.P., Rovithakis, G.A.: Prescribed performance adaptive control of siso feedback linearizable systems with disturbances. In: 2008 16th Mediterranean Conference on Control and Automation, pp. 1035–1040 (2008-06). <https://doi.org/10.1109/MED.2008.4601971>
- [30] Bu, X.: Prescribed performance control approaches, applications and challenges: A comprehensive survey. *Asian Journal of Control* **25**(1), 241–261 (2023) <https://doi.org/10.1002/asjc.2765>
- [31] Zhang, J.-X., Xu, K.-D., Wang, Q.-G.: Prescribed performance tracking control of time-delay nonlinear systems with output constraints. *IEEE/CAA Journal of Automatica Sinica* **11**(7), 1557–1565 (2024-07) <https://doi.org/10.1109/JAS.2023.123831>
- [32] Zhang, C.-L., Guo, G., Liu, Y.-X., Yang, G.-H.: Low-complexity prescribed performance control of nonlinear systems with full-state constraints. *IEEE Transactions on Circuits and Systems II: Express Briefs* **71**(4), 2254–2258 (2024-04) <https://doi.org/10.1109/TCSII.2023.3341351>
- [33] Zhang, J.-X., Chai, T.: Global prescribed performance control of unknown strict-feedback systems with quantized references. *IEEE Transactions on Systems, Man, and Cybernetics: Systems* **53**(10), 6257–6267

(2023-10) <https://doi.org/10.1109/TSMC.2023.3281982>

- [34] Wang, X., Jiang, Y., Yang, J., Yan, Y., Li, S.: Prescribed performance motion control: A control barrier function approach. *IEEE Transactions on Industrial Electronics* **71**(12), 16377–16387 (2024-12) <https://doi.org/10.1109/TIE.2024.3384527>
- [35] Xie, H., Jing, Y., Zhang, J.-X., Dimirovski, G.M.: Low-complexity tracking control of unknown strict-feedback systems with quantitative performance guarantees. *IEEE Transactions on Cybernetics* **54**(10), 5887–5900 (2024-10) <https://doi.org/10.1109/TCYB.2024.3390440>
- [36] Dimanidis, I.S., Bechlioulis, C.P., Rovithakis, G.A.: Output feedback approximation-free prescribed performance tracking control for uncertain mimo nonlinear systems. *IEEE Transactions on Automatic Control* **65**(12), 5058–5069 (2020-12) <https://doi.org/10.1109/TAC.2020.2970003>
- [37] Wang, L., Qi, R., Jiang, B.: Adaptive fault-tolerant optimal control for hypersonic vehicles with state constrains based on adaptive dynamic programming. *Journal of the Franklin Institute* **361**(8), 106833 (2024) <https://doi.org/10.1016/j.jfranklin.2024.106833>
- [38] Liu, G., Park, J.H., Xu, H., Hua, C.: Reduced-order observer-based output-feedback tracking control for nonlinear time-delay systems with global prescribed performance. *IEEE Transactions on Cybernetics* **53**(9), 5560–5571 (2023-09) <https://doi.org/10.1109/TCYB.2022.3158932>
- [39] Sui, S., Chen, C.L.P., Tong, S.: Finite-time adaptive fuzzy prescribed performance control for high-order stochastic nonlinear systems. *IEEE Transactions on Fuzzy Systems* **30**(7), 2227–2240 (2022-07) <https://doi.org/10.1109/TFUZZ.2021.3077317>
- [40] Sun, K., Guo, R., Qiu, J.: Fuzzy adaptive switching control for stochastic systems with finite-time prescribed performance. *IEEE Transactions on Cybernetics* **52**(9), 9922–9930 (2022-09) <https://doi.org/10.1109/TCYB.2021.3129925>
- [41] Song, Y., Zhou, S.: Neuroadaptive control with given performance specifications for mimo strict-feedback systems under nonsmooth actuation and output constraints. *IEEE Transactions on Neural Networks and Learning Systems* **29**(9), 4414–4425 (2018-09) <https://doi.org/10.1109/TNNLS.2017.2766123>
- [42] Gao, Z., Zhang, Y., Guo, G.: Finite-time fault-tolerant prescribed performance control of connected vehicles with actuator saturation. *IEEE Transactions on Vehicular Technology* **72**(2), 1438–1448 (2023-02) <https://doi.org/10.1109/TVT.2022.3209802>
- [43] Li, B., Gong, W., Yang, Y., Xiao, B.: Distributed fixed-time leader-following formation control for multiquadrotors with prescribed performance and collision avoidance. *IEEE Transactions on Aerospace and Electronic Systems* **59**(5), 7281–7294 (2023-10) <https://doi.org/10.1109/TAES.2023.3289480>
- [44] Zhu, C., Yang, C., Jiang, Y., Zhang, H.: Fixed-time fuzzy control of uncertain robots with guaranteed transient performance. *IEEE Transactions on Fuzzy Systems* **31**(3), 1041–1051 (2023-03) <https://doi.org/10.1109/TFUZZ.2022.3194373>
- [45] Sun, W., Yuan, J., Yang, X.: Fixed-time prescribed performance control method for nonlinear systems with unknown time-varying parameters. *IET Control Theory & Applications* **18**(13), 1751–1762 (2024) <https://doi.org/10.1049/cth2.12723>

- [46] Yang, P., Su, Y., Zhang, L.: Proximate fixed-time fault-tolerant tracking control for robot manipulators with prescribed performance. *Automatica* **157**, 111262 (2023-11) <https://doi.org/10.1016/j.automatica.2023.111262>
- [47] Wang, Z., Ma, J., Hu, L.: Predefined-time guaranteed performance attitude takeover control for non-cooperative spacecraft with uncertainties. *International Journal of Robust and Nonlinear Control* **33**(13), 7488–7509 (2023) <https://doi.org/10.1002/rnc.6761>
- [48] Yao, Y., Tan, J., Yao, Y., Zhang, X., Chen, P.: Prescribed-time prescribed performance control for stochastic nonlinear input-delay systems with arbitrary bounded initial error. *Neurocomputing* **571**, 127200 (2024-02) <https://doi.org/10.1016/j.neucom.2023.127200>
- [49] Bu, X., Jiang, B., Feng, Y.: Hypersonic tracking control under actuator saturations via readjusting prescribed performance functions. *ISA Transactions* **134**, 74–85 (2023) <https://doi.org/10.1016/j.isatra.2022.08.016>
- [50] Yao, Y., Kang, Y., Zhao, Y., Li, P., Tan, J.: Flexible prescribed performance output feedback control for nonlinear systems with input saturation. *IEEE Transactions on Fuzzy Systems* **32**(11), 6012–6022 (2024) <https://doi.org/10.1109/TFUZZ.2024.3418772>
- [51] Wang, Y., Zhang, B., Dong, J.: Enhanced adaptive prescribed performance constrained control with safe dynamic envelope for input-saturated nonlinear system. *IEEE Transactions on Automation Science and Engineering* **22**, 15396–15407 (2025) <https://doi.org/10.1109/TASE.2025.3569539>
- [52] Wang, L., Qi, R., Wen, L., Jiang, B.: Adaptive multiple-model-based fault-tolerant control for non-minimum phase hypersonic vehicles with input saturations and error constraints. *IEEE Transactions on Aerospace and Electronic Systems* **59**(1), 519–540 (2023) <https://doi.org/10.1109/TAES.2022.3185576>
- [53] Eliker, K., Jouffroy, J.: A robust quadrotor attitude controller with physical and virtual input saturations. *Aerospace Science and Technology* **163**, 110305 (2025) <https://doi.org/10.1016/j.ast.2025.110305>
- [54] Tee, K.P., Ge, S.S., Tay, E.H.: Barrier lyapunov functions for the control of output-constrained nonlinear systems. *Automatica* **45**(4), 918–927 (2009-04) <https://doi.org/10.1016/j.automatica.2008.11.017>
- [55] Hardy, G.H., Littlewood, J.E., Pólya, G.: Inequalities, 2nd edn. Cambridge University Press, Cambridge (1952). <https://www.cambridge.org/core/books/inequalities/228DDF75333B210F6A7E8D02C2DD62F5>
- [56] Tee, K.P., Ge, S.S., Tay, E.H.: Barrier lyapunov functions for the control of output-constrained nonlinear systems. *Automatica* **45**(4), 918–927 (2009-04) <https://doi.org/10.1016/j.automatica.2008.11.017>

## Statements and Declarations

### Funding

This work is supported by the National Key Research and Development Program of China (2023YFC3008802), the National Natural Science Foundation of China (52075465), and the Key Products of Hunan Province's Manufacturing Industry "Unveiled and Leading" Project (2023GXGG018), the Project of Scientific Research Fund of the Hunan Provincial Science and Technology Department (2023JJ50021, 2023GK2029, No.2024JC1003, No.2024JJ1008, 2024JJ2051, 2023GK2026), "Algorithmic Research on Mathematical Common Fundamentals" Program for Science and Technology Innovative Research Team in Higher Educational Institutions of Hunan Province of China, the Hunan Provincial Department of Education Excellent Youth Program (23B0162).

## **Conflicts of Interest**

The authors declare no conflict of interest.

## **Author contribution**

Shuli Liu: Writing-Original Draft, Methodology, Software, Visualization, Data curation. Yi Liu:Resources, Investigation, Formal analysis, Conceptualization, Writing-Review & Editing. Jingang Liu: Project administration, Validation, Funding acquisition, Writing-Review & Editing. Yin Yang: Supervision, Funding acquisition, Writing-Review & Editing. All authors have reviewed and approved the final version of the manuscript.

## **Data Availability**

The data that support the findings of this study are available from the corresponding author upon reasonable request.